

Czech University of Life Sciences Prague
Faculty of Environmental Sciences
Department of Water Resources and Environmental Modelling



Diploma Thesis

**Effect of particle size distribution in pressure drop
for inclined settling aqueous slurry flows**

B.Sc. Ormira Domnori

© 2020 CULS Prague

CZECH UNIVERSITY OF LIFE SCIENCES PRAGUE

Faculty of Environmental Sciences

DIPLOMA THESIS ASSIGNMENT

B.Sc. Ormira Domnori

Landscape Engineering
Environmental Modelling

Thesis title

Effect of Particle size distribution in pressure drop for inclined settling aqueous slurry flows in pipes

Objectives of thesis

Research regarding two phase flows are currently of high interest for the industry. We are faced with this type of flow in agriculture, food industry, oil and gas, chemical-mechanical industry, etc. Due to the lack of a database regarding this type of flow, it is crucial to do different experiments and study the flow mechanisms which affect its behavior, particularly the three types of losses and particles distribution in the pipe. In the literature there is currently considerable research, so the specific aim of this study will be to check whether the slurry flow is sensitive to particle size distribution : we will compare cases of broadly and narrow-graded sand slurry and try to quantify these slight/great changes.

Methodology

This study will use previous experimental data on two-phase flow carried out at the Hydrodynamic Institute of Prague, and models introduced in the literature, which are used to predict such behavior. Also, for this study new experiments were carried out as well, using broadly graded sand, at same flow characteristics: velocity and inclination angle, with the owns used in narrow graded sand, in order to do the comparison. We used a U-tube laboratory test loop on a range of inclinations from -45 to +45. The previous research show that the flow stratification is dependent on inclination angle sign (positive or negative). Simultaneously, a proper model with multiple particle fractions from literature is used for forecasting, it is calibrated and validated from the experimental data we have. Both experimental and model results are compared to one another.

The proposed extent of the thesis

xx

Keywords

two-phase flow, settling slurry, pressure losses, particle size distribution

Recommended information sources

1. Matoušek, V., Krupička, J., Konfršt, J., and Vlasák, P. (2019). Anomalous pressure drop in settling slurry flow through pipe of mild negative slope. Proc. 19th Int. Conference on Transport & Sedimentation of Solid Particles, Cape Town, RSA.
2. Matoušek, V., Krupička, J., Konfršt, J., and Vlasák, P. (2019). Effect of pipe inclination on solids distribution in partially stratified slurry flow. Proc. ASME-JSME-KSME 2019 Joint Fluids Eng. Conf. AJKFLUIDS2019, San Francisco, USA, paper No. AJKFLUIDS2019-5397.
3. Matoušek, V., Krupička, J., and Kesely, M. (2018). A layered model for inclined pipe flow of settling slurry. Powder Technology, 333, 317-326

Expected date of thesis defence

2019/20 SS – FES

The Diploma Thesis Supervisor

prof. Dr. Ing. Václav Matoušek

Supervising department

Department of Water Resources and Environmental Modeling

Electronic approval: 19. 3. 2020

doc. Ing. Martin Hanel, Ph.D.

Head of department

Electronic approval: 20. 3. 2020

prof. RNDr. Vladimír Bejček, CSc.

Dean

Prague on 28. 03. 2020

Declaration

I declare that I have worked on my diploma thesis titled " Effect of particle size distribution in pressure drop for inclined settling aqueous slurry flows" by myself and I have used only the sources mentioned at the end of the thesis. As the author of the diploma thesis, I declare that the thesis does not break copyrights of any third person.

This thesis was carried out at Czech University of Life Sciences in cooperation with Institute of Hydrodynamics of Czech Academy of Sciences.

In Prague on June 30th, 2020

Acknowledgement

Pursuing my studies in a foreign country has not been an easy task but writing this diploma thesis is solid evidence that I have managed to overcome the struggles in the journey. This result would not have been possible without the support of my professors, colleagues, friends, and family, so I want to express a great appreciation to everyone that has assisted me during these years.

I would like to thank all professors and lecturers of the Department of Water Resources and Environmental Modelling, that have provided guidance to me through their courses and not only. It has been a pleasure going together through the lectures, assignments, and extra-curricular activities as well.

My profound gratitude goes particularly to my supervisor, prof. Dr. Ing. Václav Matoušek, whom I have looked upon as a great scientist, professor, and human being above all. He has been encouraging, assisting and helping me all the way long. Professor Matoušek has given me the opportunity to build the foundations of my career, by making me part of the enormous ongoing work he has been doing regarding two-phase flow transportation, throughout his academic life. He showed me the beauty of Hydrodynamics through his guidance. I was blessed to be his student during this time.

The dearest gratefulness is for the most important people in my life, my close family, for caring and supporting me forever. They are the foundation of who I am and will ever be. I want to show a great appreciation to my life partner, who has been by my side all these years, always loving, supporting, and motivating me to go forward. In addition, I also want to mention my best friends and my dear university colleague, who have added fun and laughter to my journey with their constant company and support.

Finally, I want to express my sincere acknowledgement to the Visegrad Fund for financing my studies. The support they have given me, and many colleagues, is noble, and I hope they will continue their mission for a long time.

Effect of particle size distribution in pressure drop for inclined settling aqueous slurry flows

Abstract

This diploma thesis discusses the transport of liquid-solid mixtures in pipelines. The research is concentrated in the effect of particle gradation on the behaviour of inclined flows, including frictional or manometric pressure drops and the solids' stratification within the pipe. A pragmatic approach was followed to produce the full content of this thesis; that includes experiments, comparative research, and empirical modelling. The study of slurry flow mechanisms is supported with experimental results which include velocity and pressure differential measurements, concentration profiles and particle size distribution curves. The findings support the general idea that slurry flow is sensitive to the inclination angle and show a significant susceptibility of the flow to the gradation of solid particles. Broadly graded mixtures exhibit lower pressure gradients compared to narrow graded ones, and this is highly related to solids distributions within the pipe. Existing two-layered model for prediction of slurry behaviour in inclined pipes is analysed and modified for broadly graded material, using empirical correlations.

Keywords: settling slurry, inclined flow, pressure losses, particle size distribution, broad grading, experiment, model.

Vliv distribuce pevných částic na tlakové ztráty třením při proudění hrubozrnných suspenzí v nakloněném potrubí

Abstrakt

Tato diplomová práce se zabývá transportem suspenzí tvořených směsí pevných částic a nosné kapaliny v potrubí. Výzkum je zaměřen na vliv různorodých frakcí částic na režim proudění v nakloněném potrubí, včetně dopadů na tlakové ztráty absolutní, či manometrické a stupeň stratifikace proudících pevných částic v příčném profilu potrubí. Pro zpracování diplomové práce byl zvolen pragmatický přístup, který se skládá z experimentálního měření, porovnání výsledků a empirického modelování. Závěry studie se opírají o poznatky z experimentální kampaně, jejíž výstupy obsahují informace o tlakových ztrátách, rychlosti proudění, distribuci velikosti částic a koncentračních profilech částic. Závěry studie potvrzují předpoklad, že proudění směsí je závislé na úhlu náklonu potrubí a zároveň je do značné míry ovlivněno zrnitostním složením pevných částic. Směsi s širokým zrnitostním složením částic vykazují menší tlakovou ztrátu třením, než směsi tvořené úzkou frakcí pevných částic. Toto chování je do značné míry spjata s rozvrstvením pevných částic v příčném profilu proudění. Dvouvrstvý predikční model vhodný pro modelování proudění v nakloněném potrubí byl analyzován a rozšířen o empirické vztahy, které lépe popisují proudění směsí s širokým zrnitostním složením.

Klíčová slova: hrubozrnné suspenze, proudění v nakloněném potrubí, tlakové ztráty třením, koncentrační profil, široké zrnitostní složení, experiment, model.

Table of Contents

1	Introduction	1
1.1	Outline	3
2	Literature review	4
2.1	Two-phase flows: Slurries	4
2.1.1	Application of slurry transport	5
2.1.2	Environmental impact of slurry transport systems	6
2.2	Review of slurry mechanics	6
2.2.1	Mean velocity in a pipeline	7
2.2.2	Forces acting on a particle.....	7
2.2.3	Lift and drag forces	8
2.2.4	Density of the fluid.....	8
2.2.5	Deposition velocity	8
2.2.6	Settling of particles in a fluid.....	9
2.2.7	Dynamic Viscosity Equation	9
2.2.8	Concentration of solids	10
2.2.9	Pressure losses in the pipe.....	10
2.2.10	Friction gradient	11
2.2.11	Swamee-Jain equation.....	12
2.3	Classification of slurries	12
2.4	Non-horizontal slurry flows	13
2.4.1	Vertical slurry flow	13
2.4.2	Inclined slurry flow	14
2.4.3	Particle size effect on flow parameters	15
2.4.4	Particle size distribution curve	15

2.5	Worster-Denny approach on hydraulic gradient estimation.....	16
2.6	The two-layered model scheme.....	16
3	Review of existing narrow graded mixture experimental results.....	19
3.1	Anomalous pressure drops in descending flow of narrow graded sand-water mixture	19
3.2	Force balance analysis in inclined slurry flow	20
4	Methods.....	22
4.1	Experimental facility	22
4.2	Tested mixture specifications	23
4.3	Analysis of the data	25
5	Results and discussion of experimental results.....	26
5.1	Solids concentration in the pipe	26
5.2	Concentration profiles	27
5.3	Hydraulic pressure gradient.....	29
6	Comparison of broadly graded and narrow graded sand-water flow.....	31
6.1	Anomalous element in the concentration profiles	35
7	Modelling slurry flow	37
7.1	Worster-Denny prediction of frictional pressure losses	37
7.1.1	Empirical modification of Worster-Denny formula for friction gradient 38	
7.2	Two-layered model.....	40
7.2.1	The fundamental equations	41
7.2.2	Original results of the IILM for prediction of inclined broadly graded slurry flow behaviour	45
7.2.3	Results' analysis.....	49
7.2.4	Particle size effect to model performance	51
7.2.5	Findings.....	58

8	Conclusions and Recommendations	59
9	References	61

List of figures

Figure 2. 1 Profile of a vertical U-loop (Wilson, et al., 2006).....	14
Figure 2. 2 Pipeline system with no elevation difference between inlet and outlet (Matoušek, 2019)	15
Figure 2. 3 Pipeline system with elevation difference between inlet and outlet (Matoušek, 2019)	15
Figure 2. 4 Structure of settling slurry flow (Settling slurries advanced topics, Wilson, 2006)	17
Figure 2. 5 Force balance in a longitudinal cross section of the in horizontal pipe based on two layered model.....	18
Figure 3. 1 Force balance of slurry flow in ascending pipe based on two layered model	21
Figure 3. 2 Force balance of slurry flow in descending pipe based on two-layered model.....	21
Figure 4. 1 Particle size distribution curve of three narrow graded sand samples, which compose the broadly graded sand	24
Figure 4. 2 Particle size distribution curve of broadly graded sand (fraction code = S063025)	24
Figure 4. 3 Data processing steps.....	25
Figure 5. 1 Experimentally determined volumetric concentrations of solids in sand-water flow at $V_m \approx 2.5$ m/s and $C_{vd} \approx 0.24$ at different inclination angles. Legend: square marker: Spatial volumetric concentration C_{vi} ; x-marker: Delivered volumetric concentration C_{vd} .	26
Figure 5. 2 Measured solids distributions in broadly graded sand-water flow at $V_m \approx 2.5$ m/s and $C_{vd} \approx 0.24$ at inclination angles from 0 degree (upper-left plot) to ± 45 degrees (down-right plot). Legend: red o-line: narrow graded sand-water test; blue d-line: broadly graded sand-water test	28
Figure 5. 3 Layering of particles at the bottom of the pipe, clear horizontal section; no flow condition.	29
Figure 5. 4 Different hydraulic gradients (dimensionless pressure drop) in sand-water flow at $V_m \approx 2.5$ m/s and $C_{vd} \approx 0.24$ at different inclination angles. Legend: black	

square marker: measured manometric gradient; black x-line: frictional gradient from measurements	30
Figure 6. 1 Mean velocity in the pipe comparison; Legend: b-line: broadly graded; r-line: narrow graded	31
Figure 6. 2 Measured solids distributions in sand-water flow at $V_m \approx 2.5$ m/s and $C_{vd} \approx 0.24$ at horizontal flow. Legend: red circle: narrow graded sand-water test; blue diamond: broadly graded sand-water test	32
Figure 6. 3 Measured solids distributions in sand-water flow at $V_m \approx 2.5$ m/s and $C_{vd} \approx 0.24$ at positive inclination angles. Legend: red circle: narrow graded sand-water test; blue diamond: broadly graded sand-water test.....	33
Figure 6. 4 Measured solids distributions in sand-water flow at $V_m \approx 2.5$ m/s and $C_{vd} \approx 0.24$ at negative inclination angles from -5 to -45 degrees. Legend: red circle: narrow graded sand-water test; blue diamond: broadly graded sand-water test	34
Figure 7. 1 Different hydraulic gradients (dimensionless pressure drop) in sand-water flow at $V_m \approx 2.5$ m/s and $C_{vd} \approx 0.24$ at different inclination angles. Legend: black square marker: measured manometric gradient; black x-line: frictional gradient from measurements; blue o-line: manometric pressure gradient from Worster-Denny formula based on C_{vd} ; green diamond-line: manometric pressure gradient from Worster-Denny formula based on C_{vi} ; green x-line: frictional gradient by Worster-Denny based on C_{vi}	37
Figure 7. 2 Modification of Worster-Denny formula to predict friction losses. Legend: black square marker: measured friction gradient; blue x-line: frictional gradient from modified Worster-Denny; red-line: error between measured and calculated friction gradient.....	38
Figure 7. 3 Modification of Worster-Denny formula to predict friction losses. Legend: black square marker: measured friction gradient; blue x-line: frictional gradient from modified Worster-Denny; red-line: error between measured and calculated friction gradient.....	39
Figure 7. 4 Modification of Worster-Denny formula to predict friction losses. Legend: black square marker: measured friction gradient; blue x-line: frictional gradient from modified Worster-Denny; red-line: error between measured and calculated friction gradient.....	39

Figure 7. 5 Frictional hydraulic gradient (on the left) & Spatial volumetric concentration (on the right) in sand-water flow at $V_m \approx 2.5$ m/s and $C_{vd} \approx 0.24$ at different inclination angles, $C_{mode} = 1$. Legend: blue diamond marker: measured friction gradient; green plus marker: IILM (two-layered model) results. 45

Figure 7. 6 Solids concentration profile of sand-water flow at $V_m \approx 2.5$ m/s and $C_{vd} \approx 0.24$ at different inclination angles, $C_{mode} = 1$. Legend: black square marker: measured solids concentration; green-line: modelled solids concentration. 46

Figure 7. 7 Frictional hydraulic gradient (on the left) & Spatial volumetric concentration (on the right) in sand-water flow at $V_m \approx 2.5$ m/s and $C_{vd} \approx 0.24$ at different inclination angles, $C_{mode} = 2$. Legend: blue diamond marker: measured friction gradient; green plus marker: IILM (two-layered model) results. 47

Figure 7. 8 Solids concentration profile of sand-water flow at $V_m \approx 2.5$ m/s and $C_{vd} \approx 0.24$ at different inclination angles, $C_{mode} = 2$. Legend: black square marker: measured solids concentration; green-line: modelled solids concentration. 48

Figure 7. 9 Results for different friction gradients and spatial volumetric concentrations, of sand-water flow, at $V_m \approx 2.5$ m/s and $C_{vd} \approx 0.24$, at different inclination angles, with $transpEq = 1$; $C_{mode} = C_{vd}$; Legend : black-square: Measured frictional hydraulic gradient; green-diamond: $fricEq = 2$; blue-back-arrow: $fricEq = 3$; black-x: $fricEq = 5$; yellow-up-triangle: $fricEq = 6$; cyan-plus: $fricEq = 9$; red-down-triangle: $fricEq = 10$; 49

Figure 7. 10 Results for different friction gradients and spatial volumetric concentrations, of sand-water flow, at $V_m \approx 2.5$ m/s and $C_{vd} \approx 0.24$, at different inclination angles, with $transpEq = 2$; $C_{mode} = 1$; Legend : black-square: Measured frictional hydraulic gradient; green-diamond: $fricEq = 2$; blue-back-arrow: $fricEq = 3$; blue-circle: $fricEq = 4$; black-x: $fricEq = 5$; yellow-up-triangle: $fricEq = 6$; cyan-plus: $fricEq = 9$; red-down-triangle: $fricEq = 10$; 49

Figure 7. 11 Results for different friction gradients and delivered volumetric concentrations, of sand-water flow, at $V_m \approx 2.5$ m/s and $C_{vd} \approx 0.24$, at different inclination angles, with $transpEq = 1$, $C_{mode} = 2$; Legend: black-square: Measured frictional hydraulic gradient; green-diamond: $fricEq = 2$; yellow-up-triangle: $fricEq = 6$; cyan-plus: $fricEq = 9$; red-down-triangle: $fricEq = 10$; 50

Figure 7. 12 Results for different friction gradients and delivered volumetric concentrations, of sand-water flow, at $V_m \approx 2.5$ m/s and $C_{vd} \approx 0.24$, at different inclination angles, with $transpEq = 2$, $C_{mode} = 2$; Test with $transpEq = 2$; Legend: black-square: Measured frictional hydraulic gradient; green-diamond: $fricEq = 2$; blue-back-arrow: $fricEq = 3$; yellow-up-triangle: $fricEq = 6$; cyan-plus: $fricEq = 9$; red-down-triangle: $fricEq = 10$;..... 50

Figure 7. 13 Results for different friction gradients and delivered volumetric concentrations, of sand-water flow, at $V_m \approx 2.5$ m/s and $C_{vd} \approx 0.24$, at different inclination angles, with $transpEq = 2$, $C_{mode} = 1$, $fricEq = 2$; Legend: black-square Measured frictional hydraulic gradient/ C_{vi} ; green-square: d_{50} ; magenta-diamond: d_{30} ; cyan-circle: d_{75} 51

Figure 7. 14 Solids concentration profile of sand-water flow at $V_m \approx 2.5$ m/s and $C_{vd} \approx 0.24$ at different inclination angles, with $transpEq = 2$, $C_{mode} = 1$, $fricEq = 2$; Legend: black-square: measured concentration profile; green-square: d_{50} ; magenta-diamond: d_{30} ; cyan-circle: d_{75} 52

Figure 7. 15 Results for different friction gradients and delivered volumetric concentrations, of sand-water flow, at $V_m \approx 2.5$ m/s and $C_{vd} \approx 0.24$, at different inclination angles, with $transpEq = 2$, $C_{mode} = 1$, $fricEq = 6$; Legend: black-square Measured frictional hydraulic gradient/ C_{vi} ; green-square: d_{50} ; magenta-diamond: d_{30} ; cyan-circle: d_{75} 53

Figure 7. 16 Solids concentration profile of sand-water flow at $V_m \approx 2.5$ m/s and $C_{vd} \approx 0.24$ at different inclination angles, with $transpEq = 2$, $C_{mode} = 1$, $fricEq = 6$; Legend: black-square: measured concentration profile; green-square: d_{50} ; magenta-diamond: d_{30} ; cyan-circle: d_{75} 54

Figure 7. 17 Results for different friction gradients and delivered volumetric concentrations, of sand-water flow, at $V_m \approx 2.5$ m/s and $C_{vd} \approx 0.24$, at different inclination angles, with $transpEq = 2$, $C_{mode} = 1$, $fricEq = 9$; Legend: black-square Measured frictional hydraulic gradient/ C_{vi} ; green-square: d_{50} ; magenta-diamond: d_{30} ; cyan-circle: d_{75} 55

Figure 7. 18 Solids concentration profile of sand-water flow at $V_m \approx 2.5$ m/s and $C_{vd} \approx 0.24$ at different inclination angles, with $transpEq = 2$, $C_{mode} = 1$, $fricEq = 9$

9; Legend: black-square: measured concentration profile; green-square: d50; magenta-diamond: d30; cyan-circle: d75..... 56

List of tables

Table 4. 1 Sand particle analysis.....	23
Table 7. 1 Frictional hydraulic gradient mean error (measured vs. modelled) for 10 mm pipe test of sand-water flow at $V_m \approx 2.5$ m/s and $C_{vd} \approx 0.24$.	57
Table 7. 2 Distributed/Spatial volumetric concentration mean error (measured vs. modelled) for 10 mm pipe test of sand-water flow at $V_m \approx 2.5$ m/s and $C_{vd} \approx 0.24$	57

List of abbreviations

A	cross-sectional area of pipe (m^2)
B_s	constant in friction law for hydraulically rough boundary
c	local volumetric concentration
C_b, C_a	mean spatial volumetric concentration in the bed, in area above bed respectively
C_{vd}	mean delivered volumetric concentration
C_{vi}	mean spatial volumetric concentration in entire pipe cross section
d_{50}	mass-median diameter of particle (m)
D	inner diameter of pipe (m)
g	gravitational acceleration (m/s^2)
i	hydraulic gradient
k_s	equivalent roughness of the top of the bed (m)
L	length of pipe (m)
O	perimeter (m)
p	pressure (Pa)
q_s	volumetric transport rate for unit width (m^2/s)
Q	volumetric flow rate (m^3/s)
Re_p	particle Reynolds number
R_h	hydraulic radius (m)
S	relative density
V	mean velocity of flow (m/s)
w_t	terminal settling velocity of solid particle (m/s)
y	vertical position above bottom of pipe (m)
α	empirical coefficient in solids transport formula
β	empirical coefficient in solids transport formula
θ	Shields parameter (dimensionless shear stress) for bed
κ	Karman constant
λ	Darcy-Weisbach friction coefficient
ν_f	kinematic viscosity of fluid (m^2/s)
ρ	density of fluid (kg/m^3)
τ	shear stress at flow boundary (Pa)

Φ Einstein transport parameter
 ω angle of pipe inclination

Subscripts:

f, m, s fluid, mixture, solids
fric, man frictional, manometric
w wall
 ω inclined

1 Introduction

This diploma thesis is a comprehensive summary of my one-year research study on slurries. Slurries are the multiphase mixtures flowing through pipes of different parameters and for various purposes. The most common involve water or oil as their carrying liquid and are linked respectively to the hydrodynamic or oil and gas industries.

Study of slurries is strongly linked to the study of fluids and solids but more importantly, to changes in their behaviour when put together in motion. My research commenced as an investigation and assessment of the currently available literature on this topic, and it has been strongly influenced by the work of remarkable researchers, such as K. C. Wilson, C. A. Shook, my professor V. Matoušek, and others mentioned in references. Even though natural slurry flow has always been part of the environment, the necessity to carefully study its behaviour was raised in the 20th century, simultaneously with the industrial developments all over the globe. Today, tons of slurry are transported in industrial pipelines, contributing to the chain of elements which simplify our lifestyle and make it convenient for the 21st century.

Before starting this work, given the fact that V. Matoušek was my professor at the university, I was able to learn the basics of this topic and note how much more progress is to be accomplished in this field. For some decades, scientists and engineers have been conducting experiments and making analysis of the slurry behaviour; thus, there are a lot of known theories and equations, but the whole picture is still uncertain.

Slurries are a broad category of mixtures with different characteristics. Furthermore, when used in several locations and for many purposes, they are transported through pipelines of various parameters like the diameter, roughness, length and inclination angles. There are only a few facilities in the world which can do experiments on slurries, and most of them have different specifications. One of these facilities is located at the Institute of Hydrodynamics in Prague, and a lot of experiments have been carried out in the premises of this institution, which is part of the Czech Academy of Science. The experimental work is done in a U-loop laboratory pipeline, connected to a very powerful centrifugal pump, as required for such conditions. During the summer of 2019, I was given a chance to be part of the team that conducts the

experiments, and I was able to produce new data on slurry flow. Different from common practice, my research is focused on inclined flow (there exist more uncertainty and lack of knowledge), and the broad gradation of solid particles. Most experiments implement just a mean size of particles without taking into consideration any effect of particle gradation on slurry flow performance. Hence, I believe that the findings of this research will have a substantial impact on further slurry studies.

During the past few decades, in order to help engineers, meteorologists, economists, and other professionals in the decision-making process, models are being used. A model is a tool which resembles a given situation based on some parameters and inputs and is able to predict or forecast the results of a slightly different situation created by other inputs. Modelling has proved to be a beneficial tool in complex systems, being weather forecast, economic predictions, structure design, environment management, etc. Models are used by our computers and mobile phones, which makes it an important part of daily activities, even if it is not really noticed. That being said, it is clear that despite studying and understanding some natural or human-made event, it is also crucial to construct a model which would reproduce the original results in the most explanatory manner.

Some well-known formulas or models are currently being used to predict the behaviour of slurry flow; however, they have certain limitations. My research is focused on inclined flows with broadly graded material, and both these specifications represent a challenge for modellers. Mechanisms governing flow friction and particles' interaction at the same time are not well understood, so an accurate prediction, in this case, becomes uncertain. Having the opportunity to produce experimental data of broadly graded slurry flow in different inclinations, I continued my study on producing satisfying predictions of this flow on the basis of existing approaches.

Coming from a civil engineering background, I understand how challenging a design process can be if there is a lack of a certain amount of information. Pipeline designs acquire precise information on pressure drop, critical velocity, flow regimes and much more. Thus, with this research aims to broaden the existing database of information on slurries and introduce a model which is able to accurately predict the slurry flow behaviour in certain conditions.

1.1 Outline

The structure of this thesis allows readers with and without good information on the topic to follow the text. It starts with a general description of slurries and benefits of using pipelines as a mean of slurry transport. In the second chapter, I have presented a review of existing literature which is related to the methodology and objectives of this thesis. Special attention is paid to late works conducted at the Institute of Hydrodynamics in Prague, which served as groundwork for my research. The main part of the thesis shows the used methods and experimental specifications. Following that, results of conducted tests are introduced and analysed. One chapter is fully devoted to the comparison of broadly graded and narrow graded slurries, which is also a major objective of this thesis. At the end, I have analysed a few existing approaches that predict the behaviour of inclined slurry flow and I have employed them in the model to try predicting the friction gradient and concentration profiles of the slurry flow with broadly graded material. Several empirical modifications were made, and the best predictive approach is proposed for further use. My recommendations for additional future research are described in the last chapter. Finally, all used literature is mentioned as references of this thesis.

2 Literature review

2.1 Two-phase flows: Slurries

Before using the two-phase flow transportation in all industries, at the beginning of the 20th century, erosion was a unique phenomenon, where the sand and water acted together in a state of motion (Miedema and Ramsdell, 2016). In a century time, mixtures flowing together has been a subject of continuing investigation and research, with different countries conducting experimental work on handling these systems. Amongst most notable in the last century were the United States of America, Canada, United Kingdom, the Netherlands, etc., with their great teams of scientists.

Throughout the length of a century, much has changed. Hundreds of types of industries deal with water uniquely and among them at least some tens use or deal with mixtures of different phases. Any kind of fluid on its own, in a liquid state, consists of one phase. A combination of two or more states or phases creates the mixture.

Industry pipelines involve transportation of many phases of materials at once. These mixtures can be slurry, sludge, or wastewater. These names represent some solids which are being transported in a carrying liquid, and then the difference is only the size or behaviour of the solids within. Slurries, which are the matter of interest in this research work, are all liquids which contain some erosive solids in suspension (Rayner, 1995).

Scientists have been observing and understanding fluid behaviour for a long time. Pioneer of these studies was Leonardo Da Vinci, who tried to explain in a primitive way how physics of water cycle works, succeeded by Isaac Newton, Blaise Pascal, Daniel Bernoulli, all of which together have given us the foundations of nowadays' hydraulics. We possess all the fundamental equations which solve the parameters of water flowing through a pipe or river, therefore designing water pipelines is a relatively easy task, compared to designing a slurry pipeline. We do not possess the equations which accurately describes the slurry flow mechanism, so we cannot predict the parameters of the flow, which consequently makes designing a slurry pipeline a very complicated task. In order to achieve the high aim of finding the equations to solve the parameters of this flow, it is necessary to run a lot of experiments, which, itself, represents a very complex task. First, these experiments require vast amounts of

funding because it is necessary to build a special loop which will carry the slurry, and there needs to mount a very powerful centrifugal pump. It is basically a try-error scheme of an experiment, where if you fail, you block the laboratory loop, and in the worst scenario, you destroy all the expensive tools mounted there.

2.1.1 Application of slurry transport

Tremendous amounts of slurry are transported through pipes every year, mostly due to the dredging industry (cutting and adding landfill in river streams or shores), manufactures of fertilizes, and lately waste-material also makes up for a large part of the overall slurry transport, due to higher sensibility for maintaining the environment (Wilson, et al., 2006). The application of slurry transport is increasing, as it is evident to more users that it is more cost-efficient than truck-transport of mixtures (Wilson, et al., 2006). In addition to man-made structures, slurry flow is present in nature as well. While the most common case is in the bottom of rivers beds, two-phase flow occurs in lakes, reservoirs, deep sea, mud flows, or even desert sand dunes where the carrying fluid is air (Garcia, 2013). Floods are a typical example of the malfunctioning of a slurry transportation system, when the debris that is exported at the bottom of the river gets stuck and causes the river to flow above the floodplain. Studies are carried out to understand both conditions, but most of the experimental tests involve pipelines flows.

Other examples of slurries (Polanský, 2014):

- Cement slurry, a mixture of cement, water, and assorted dry and liquid additives used in the petroleum and other industries
- Soil/cement slurry, also called Controlled Low-Strength Material (CLSM), flowable fill, controlled density fill, flow able mortar, plastic soil-cement, K-Krete
- A mixture of thickening agent, oxidizers, and water used to form a gel explosive
- A mixture of pyroclastic material, rocky debris, and water produced in a volcanic eruption and known as a lahar
- A mixture of bentonite and water used to make slurry walls
- Coal slurry, a mixture of coal waste and water, or crushed coal and water
- Slurry oil, the highest boiling fraction distilled from the effluent of an FCC unit in an oil refinery. It contains large amount of catalyst, in form of sediments hence the denomination of slurry.
- A mixture of wood pulp and water used to make paper

- Manure slurry, a mixture of animal waste, organic matter, and sometimes water often known simply as "slurry" in agricultural use, used as fertilizer after ageing in a slurry pit
- Meat slurry, a mixture of finely ground meat and water, centrifugally dewatered
- An abrasive substance used in chemical-mechanical polishing
- Slurry ice, a mixture of ice crystals, freezing point depressant, and water
- A mixture of raw materials and water involved in the raw mill manufacture of Portland cement
- A mixture of minerals, water, and additives used in the manufacture of ceramics
- A composite slurry formed from a combination of no less than three of the aforementioned slurries.

2.1.2 Environmental impact of slurry transport systems

As mentioned above, the use of slurry systems has increased over the years. Today's application includes not only complex environments but also conventional transportation of bulk material in a long-distance. Comparing slurry systems to mechanical transport, the use of pipelines makes the whole process more efficient. It demands less space, requires fewer operating staff, eliminates several in-between procedures, and is controlled better (Lahiri, 2010). The efficiency is achieved by reducing the consumption of energy and water, which creates not only savings in capital investment, but it also ensures a dust-free environment. Slurry transportation systems show highly reduced impacts on human health and the environment by reducing emissions, including the dispersion of the material being transported (Wilson et al., 2006). Workers and the surrounding environments are directly exposed to the dispersion of the carried material (uranium ores or coal are among the most dangerous, commonly transported materials, according to Wilson et al., (2006)), and this is a matter of concern. There exist many studies related to the environmental and economic benefits of changing the old transportation system, which also illustrate the importance of improving hydraulic slurry transportation.

2.2 Review of slurry mechanics

A slurry comprises properties of liquids and solids, yet both affected by the presence of one another. Key parameters of slurry flow commence from the simple liquid flow

parameters, such as velocity, density, viscosity, roughness and hydraulic gradients. Turning from simple liquid flow to that of a mixture, immediately it is necessary to create a more careful treatment of the problems and have a precise system of solving the unknowns. (Wilson et al., 2006).

When the two-phase flow is discussed, or more specifically slurries, two components are identified: the carrying fluid, and carried solids (in this thesis, I will be referring to aqueous mixtures with soil material, therefore unless stated otherwise, the mentioned flow is composed of water and sand).

2.2.1 Mean velocity in a pipeline

One of the fundamental parameters in a pipeline flow is the mean velocity, which represents the volumetric flow rate over the pipeline cross-sectional area.

$$V_m = \frac{Q_m}{A} \quad (1)$$

The correct estimation of the mean velocity in a slurry flow is necessary to ensure safety and low-cost operation of the pipeline. Solid particles that compose the slurry flow tend to settle and form a bed at the bottom of the pipe, first sliding and then stationary. This process occurs when the mean velocity in the pipe decreases. On the other hand, when the mean velocity in the pipe increases, solid particles (especially small-sized) cannot settle, so together with the carrying liquid, tend to form a homogenous mixture moving very rapidly in the pipe. The slurry flow in high velocities though, if running for a long amount of time, could create abrasive erosion and degrading of the outer wear of solid particles. For practical pipeline operation, to ensure the optimum medium, the mean velocity in the pipe should be just above the threshold velocity at which solid particles sliding at the bottom of the pipe stop and form a stationary deposit. Mean pipeline velocity under that threshold can create a plug, therefore it is considered dangerous.

2.2.2 Forces acting on a particle

Before going deeper into studying slurries, it is essential to highlight the motion of single particles in the fluid itself. Slurries exhibit different behaviour according to the mixture composition and the flow parameters. In heterogeneous flows, usually

observed in slurries of large particle sizes, the particles settle at the bottom of the bed, and a mean of transportation is the support by mutual granular contact. In other flows, homogenous, or slurries with fine particles, surface forces are more significant. For larger particles, due to very strong velocity gradients and particle rotation, the lift forces are dominating as well.

2.2.3 Lift and drag forces

In any case of a body immersed in a fluid, there is an interaction between the body and the fluid surrounding it. In physics, any interaction is explained by a balance of forces involved. In this case, there are two forces at the interface of fluid and the immersed body: the viscous effect is reflected in the shear force and the pressure is reflected in the normal force at the interface. Respectively, the viscous effect is referred to as the drag force, because it is acting in the direction of the flow, and it tends to carry the immersed body in that direction as well. The pressure force, normal to the interface area, is what we call the lift force.

2.2.4 Density of the fluid

Density of the carrying liquid, in this case water, is also a very important parameter of the flow. Density of water changes with temperature, therefore it is necessary to make the calculation at every observation point. In this thesis, I am using an empirical formula for density as a function of temperature only (temperature in degree Celsius).

$$\rho = 1000 * \left(1 - \left(\frac{T + 288.9414}{508929.2 \times (T + 68.12963)} \right) * (T - 3.9863)^2 \right) \quad (2)$$

2.2.5 Deposition velocity

The deposition velocity represents a threshold velocity, at which solid particles begin to deposit at the bottom of the pipe, and a stationary bed of particles is formed. Capability to calculate the deposition velocity of slurry flow is one of the essential elements of pipeline design since it generally determines the lowest possible operating velocity. In the past academic research or industrial experience, great focus is given to the estimation of deposition velocity of a range of slurry flows. Nevertheless, much

old data is biased due to problems encountered during the experiments, some parameters of the flow were mistakenly not measured, only a small number of facilities in the world can perform such tests and overall, even today, the design of slurry pipelines counts on correlations obtained from a limited database.

2.2.6 Settling of particles in a fluid

Slurry flows are always associated with the degree of particle settling in the carrying liquid. When the density of a particle is different from the density of the fluid, in a no-flow condition, the particle moves. The particle moves up if its density is lighter or settles down if it is heavier than the carrying fluid. It is crucial in slurry flows, to estimate the velocity of the particle at which it stops moving, i.e. reaches static position. By performing a force balance at the particle, the settling velocity is determined. The particle has a weight, which is represented by the downward gravitational force; the carrying fluid (water in this thesis) inserts a hydrostatic force upwards, also known as the Archimedes buoyancy force; and the drag force, as a result of interaction between the particle and the fluid, acts downward (opposite direction with the Archimedes force). Summing up the forces, the terminal settling velocity is then calculated as a result of liquid parameters ρ_f and μ , particle diameter d , the density of the solids ρ_s , and to some extent, its shape. Many approaches exist in the literature to estimate the terminal settling velocity and a study from Albar (2000) makes a comparison among them. Another important velocity is the hindered settling velocity, which is associated with vertical slurry flows. Particles in vertical flows interact with each other and contribute to the overall density of the carrying liquid, so the hindered settling velocity of particles in this condition is lower than the average settling velocity.

2.2.7 Dynamic Viscosity Equation

Viscosity is the term which describes the fluid's resistance to flow. Dynamic viscosity is the ratio of the shear stress over the rate of shear strain. The dynamic viscosity of water is about 0.89 mPa.s at room temperature (25°C), but it changes with temperature. This is an important term when trying to understand the flow behaviour, therefore it is precisely calculated in the model, having temperature as its input. One of the most widely used empirical equations for the dynamic viscosity is the Andrade equation,

with two, three or four parameters. In my research I will be using the three-parameter equation, consisting of fitting parameters A, B and C.

$$\mu = A * 10^{\frac{B}{T-C}} \quad (3)$$

Temperature in this equation is described in degrees of Kelvin, while the values for the fitting parameters for water are: $A = 2.414 \times 10^{-5}$ Pa.s; $B = 247.8^\circ\text{K}$; $C = 140^\circ\text{K}$.

2.2.8 Concentration of solids

One of the most important parameters in slurry flows is the solids concentration in the carrying fluid. There are two different types of concentrations, based on the way how that is measured. The Volumetric spatial concentration, noted as C_{vi} in literature, the ratio of volume of particles over the total volume of the mixture. This parameter is crucial in understanding relations between other parameters of the flow such as velocity, pressure, friction, particle size, etc. C_{vi} values change with position in the pipe cross section, relatively to the top or bottom. It is a key parameter to observe the deposition limit velocity and the stratification level.

The delivered concentration on the other hand, is the ratio of discharge of particles and the discharge of total mixture. In other words, it measures the difference on the ease of transport between the carrying liquid and the solid particles.

$$C_{vd} = \frac{Q_s}{Q_m} = \frac{V_{sp}}{V_m} C_{vi} \quad (4)$$

The particles are non-uniformly distributed throughout the pipe, and often they stratify to form a solids' bed at the bottom of the pipe. Theoretically, in a stratified flow, the solids' concentration is zero at the top of the solids' bed, and it reaches higher values near the pipe wall. (Matoušek and Zrostlík, 2019)

2.2.9 Pressure losses in the pipe

For pipeline design engineers, it is essential to make the relation between the pressure drops and design parameters. Pressure drops in a slurry pipeline occur generally due to longitudinal friction and in case of vertical or inclined flow, the static component is also considered. The sum of all hydraulic gradients in a pipeline is converted to energy,

which the pumps in the system must provide. The overall pressure gradient formula originates from the Bernoulli Equation:

$$i_{m,\omega}^{\text{total}} = \frac{\Delta p_{\omega}^{\text{total}}}{L\rho_w g} = i_{m,\omega}^{\text{fric}} - S_{mi}\sin\omega \quad (5)$$

Where the relative density of the mixture is described by Matoušek et al. (2019):

$$S_{mi} = \frac{\rho_{mi}}{\rho_w} \quad (6)$$

and

$$S_{mi} = S_f + (S_s - S_f)C_{vi} \quad (7)$$

A differential pressure transmitter is used to measure all relevant pressure drops in the pipeline. The transmitter gives data for the manometric hydraulic gradient. The amount of pressure losses attributed to friction is determined later by subtracting the C_{vi} - based static part of the manometric gradient.

In slurry flows, ‘settling’ and ‘non-settling’ terms refer to two extreme conditions, while the majority of pipelines operate within a middle spectrum of flow behaviour. This fact implies that it is not an easy task to distinguish between the types of flow. However, it is generally accepted that rheology of slurries with solids’ median particle diameter more than 50-100 μm and with a low concentration of fines, is not dominated by fines effect, so a heterogeneous flow is possible (Shook, et al., 2002).

2.2.10 Friction gradient

Pressure drops in a pipeline are a result of friction losses throughout the transportation system, and of static changes in the case of non-horizontal pipes. The pressure losses attributed to friction are the unrecoverable energy loss over the pipe length. Thus, a simple way to explain the friction gradient is the difference between the manometric pressure loss and the static component:

$$i_m^{\text{fric}} = (p_1 - p_2) - \rho_m g z \quad (8)$$

Friction gradient is a typical aspect of the flow where the difference between fluid-only and slurries is encountered. The presence of a second phase changes the structure

of the flow, which exhibits higher shear stress for a given state of motion of the slurry (Shook, et al., 2002).

General equations for predicting pipeline friction gradient were firstly introduced by Newitt et al. (1955), and Durand and Condolios (1952), while more reliable equations to interpret the friction gradient were derived by Wilson K.C. in a series of publications. Wilson was the first to introduce the two-layered model, which now exists in different versions.

2.2.11 Swamee-Jain equation

Estimating pressure losses due to friction in a pressurized pipe is a crucial process in further solving of technical problems or designing a new pipeline. The widely used formula to predict these losses is the Colebrook-White equation which involves an unknown friction factor, also called the Darcy-Weisbach factor. This equation is used for turbulent flows (the usual reality case), and it is implicit; thus, some sort of numerical simulation is required to solve it. Swamee-Jain equation originates from the Jain equation of friction, but it is a simplified version of it. It includes only the term of relative roughness and Reynold's number, which are the input terms in any hydraulic model.

$$f = \frac{0.25}{\left[\log \left(\frac{\varepsilon/D}{3.7} + \frac{5.74}{\text{Re}^{(0.9)}} \right) \right]^2} \quad (9)$$

2.3 Classification of slurries

The most common terms used in two-phase flow transportation, are settling and non-settling slurry.

When the flow is considered non-settling, it is identified by a homogenous flow throughout the pipe cross-section. This condition, in general, is present in pipes operating in high velocities, so the mean velocity in the pipe is higher than the particles' settling velocity. The settling slurry flow indicates that the mean velocity in the pipe is at or lower than at least some particles' settling velocity. Depending on the

ratio of the particles that have settled at the bottom of the pipe, a new classification is developed.

A pseudo-homogenous settling flow is usually considered a Newtonian, turbulent slurry flow, where the particles are mostly moving due to turbulent suspension, and there is only a light particle concentration gradient in the pipe cross-section. Such type of flow is visible in mixtures consisting of fine solids.

A heterogenous settling flow is usually a Newtonian, turbulent slurry flow, where the particles' concentration gradient is significant, and there can be a slip between the two phases (carrying liquid and the solids). This type of flow is observed when the mixture is composed of medium particle size of solids.

Finally, the fully stratified settling flow is a Newtonian, turbulent slurry flow, where the particles' concentration gradient is very sharp due to settling of almost all particles in the mixture. The two phases are clearly distinguished. This type of flow is usually observed in coarse particles' mixtures.

2.4 Non-horizontal slurry flows

Pipelines transporting slurries have to go through different terrain. Therefore, it is impossible to maintain the horizontal flow all the way. In many sections of pipelines, we encounter inclined slurry flow, or in more rare cases, vertical slurry flow.

2.4.1 Vertical slurry flow

Pipelines of different purposes go through mountains, lakes, rivers, towns or highly populated cities. This being the case, they often include non-horizontal sections and even totally vertical ones (mostly in the mining industry). In general, vertical flows are considered non-stratified, which indicates that for all types of slurries, exhibiting stratification or not in the horizontal flow, flow in a 90° inclination angle is considered homogenous. However, individual particles may travel at local velocities that are different from the carrying liquid velocity in these vertical pipes.

Vertical pipes can transport two-phase mixtures both in upward and downward directions, and the two of them have different properties. While the delivered

volumetric concentration remains constant throughout the pipelines, the spatial volumetric concentration changes.

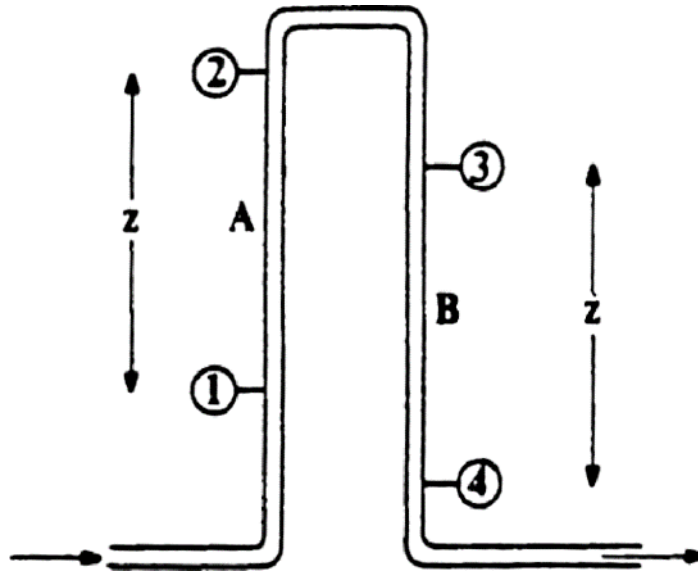


Figure 2. 1 Profile of a vertical U-loop (Wilson, et al., 2006)

2.4.2 Inclined slurry flow

Sections of the pipelines can be inclined to ranges of angles from 0 to +90 degrees, and this is mostly common in offshore and dredging industries. In general, compared to the horizontal flows, the inclined flows tend to require higher velocities in order to avoid any deposition. Previous research shows that the flow is very sensitive to the inclination angle (Matoušek et al., 2019). Generally, the existing methods for determining the hydraulic gradient in inclined pipes simply multiply the hydraulic gradient of a horizontal pipe to the cosine of a certain angle and add the static energy term, however, the inclination effect is not this simple to be determined (Miedema, 2019). To estimate the inclination effect, it is necessary to determine the flow regime, and measure the influence of the inclination angle to that specific regime.

The effect of pipe inclination on the pressure drop currently can be estimated by using two modelling approaches. One approach uses semi-empirical correlations, and the other uses layered models (typically two-layered) based originally on Wilson's principles (layered model). All these methods require an expanded database to be validated, which consists of different scenarios of slurry transportation.

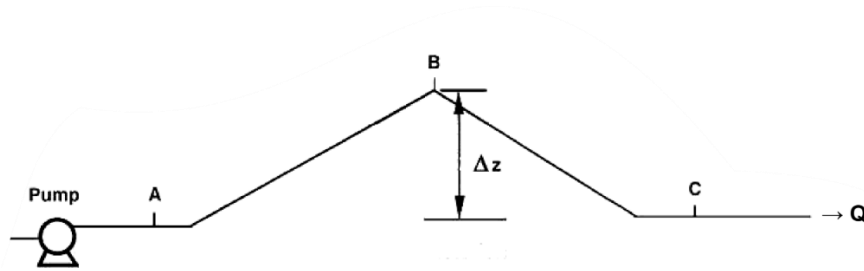


Figure 2. 2 Pipeline system with no elevation difference between inlet and outlet (Matoušek, 2019)

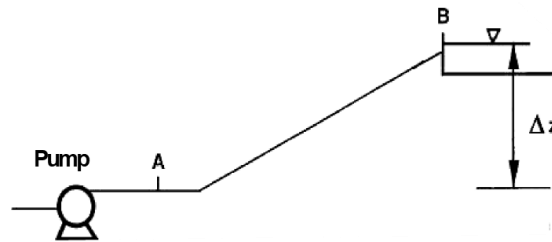


Figure 2. 3 Pipeline system with elevation difference between inlet and outlet (Matoušek, 2019)

2.4.3 Particle size effect on flow parameters

Correlations of particle size diameter and slurry flow parameters have been a subject of research discussion for many scientists who work on slurries. It has been revealed that these correlations can be represented by just a single, average particle size, or as a bimodal particle size mixture. In many industrial applications, slurries contain solids of very broad particle size distribution, which do not accurately fit in the two categories above- mentioned.

Presence and quantification of fines in a slurry flow are essential in making calculations for industrial slurries, (Gillies and Shook, 1991). In their publication, the authors suggested that the viscosity and density of the fines and liquid mixtures must be measured and used in the deposition velocity since the homogenously suspended fines increase the viscosity of the carrying liquid.

2.4.4 Particle size distribution curve

Since the need for research on slurry flows is due to high uncertainty and errors in designing pipelines, it is crucial to understand what exactly is happening in the process. Most of the fields that deal with slurries: hydrological, mining, technological, chemical, etc., are working with natural slurry components: different liquids and soil. Soil is defined as any accumulation of mineral particles due to weathering of rocks.

We can find soil particles in a range of 0.0001 mm to 100mm in diameter (Craig, 2004). Therefore, to make the findings more applicable, it was decided to carry out experiments with broadly graded sand-water slurry.

2.5 Worster-Denny approach on hydraulic gradient estimation

In a horizontal pipe, gravity tends to stratify the mixture into layers: a lower layer of solids and the upper layer of carrying liquid (Worster and Denny, 1955). Despite the regular pressure drops occurring in a water medium, the slurry flows exhibit excess friction due to solids effect. Worster and Denny formula (Worster and Denny, 1955, as cited in Wilson et al., 2006) for prediction of slurry behaviour in different inclination angles is a simple and widely used tool in this field. It is based on the behaviour of water flow and solids effect, and it is one among a small group of formulas which consider the inclination effect in the pressure drops of slurry flow. The formula suggests that in horizontal flows, the frictional solids' effect alone, generate the frictional hydraulic gradient. In inclined flows, the angle is introduced in the formula in the form of sin or cosine, which represents the cross-pipe component for submerged weight. Furthermore, the solids' effect is implemented on the static gradient in the vertical projection of the inclined pipe. Worster-Denny formula (1955) for manometric pressure drop is as follows:

$$\frac{\Delta p_{\omega}^{\text{man}}}{\rho_w g L} = i_m^{\text{man}} = i_f + (i_{m,0}^{\text{fric}} - i_f) \cos \omega + (S_s - S_f) C_{vd} \sin \omega \quad (10)$$

$$(i_m^{\text{fric}} - i_f) = (i_{m,0}^{\text{fric}} - i_f) \cos \omega \quad (11)$$

A downside of Worster-Denny approach is that by introducing the inclination effect in the friction gradient as a cosine function, it calculates the same friction losses in both limbs of the pipe, ascending and descending (negative and positive angles have same cosine).

2.6 The two-layered model scheme

Models predicting the behaviour of slurry flow, either the pressure losses, or solids' concentration profiles should be based on a logical and mathematical description of the related mechanisms. The basis of all models is the structure of the flow, usually

divided in layers. In my research, I was focused on the two layered model of slurry flow which considers the pipe cross section composed of two layers: carrying liquid at the top and solids' bed at the bottom.

As mentioned above, K.C. Wilson was the first to develop the so called two-layered model which is able to interpret slurry flow based on a two-layer scheme. This model, which has been further developed by researchers to include a wide range of application, considers a fully stratified flow in which all the particles are concentrated in the lower portion of the pipe and the Coulombic contribution to particle-wall friction is dominant (Shook, et al., 2002). Coulombic friction is the dry friction that is present in the physical interaction between two solid bodies, yet, it is very complex and remains out of the scope of this thesis. The Saskatchewan Research Council has simplified the Wilson's model to provide a general description of slurry flow, where the Coulombic contribution is significant but not dominant (Shook, et al., 2002). This version of the two-layered model is later developed in response to experimental results with a wide range of parameters.

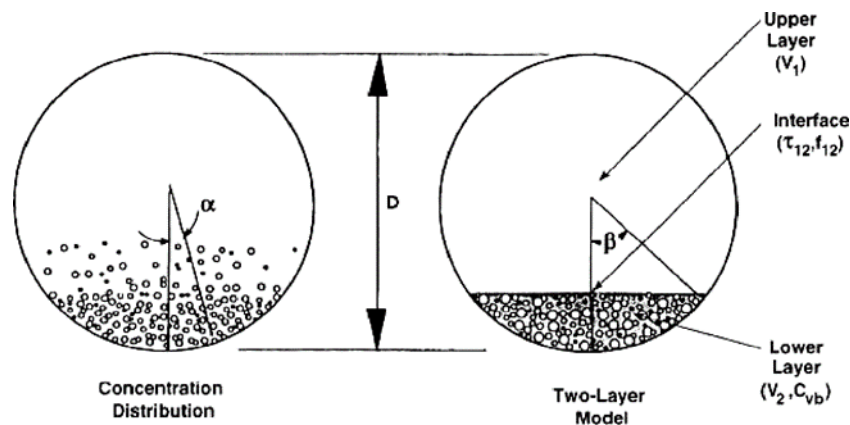


Figure 2. 4 Structure of settling slurry flow (Settling slurries advanced topics, Wilson, 2006)

The two layered model is based on balance of forces acting on each layer, dividing them in two groups: driving and resisting forces (according to their impact on a certain location), as seen in Figure 7. 2.. The stresses τ_1 and τ_{12} oppose the motion of the upper layer, while the stress τ_2 opposes the motion of the lower layer. Stress τ_{12} is a driving force on the lower layer of solids (Shook, et al., 2002). Stresses related to the pipe wall contact in the upper and lower layer respectively, τ_1 and τ_2 , are considered kinematic due to their dependence on the velocity parameter.

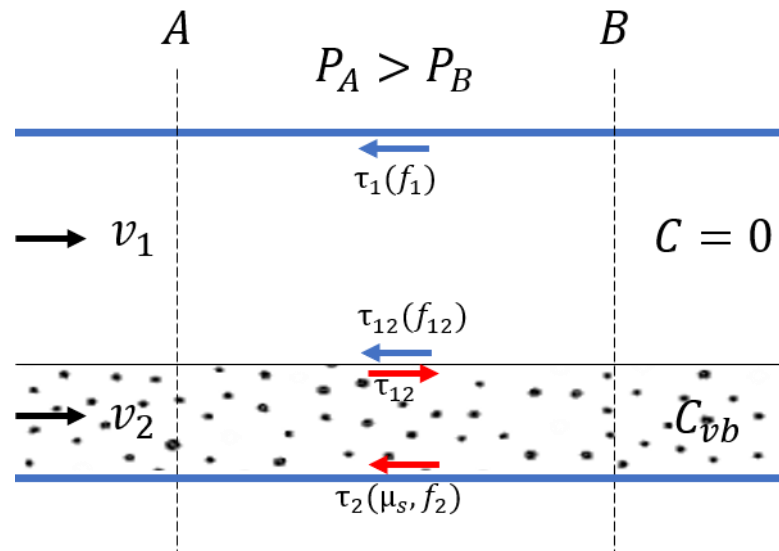


Figure 2. 5 Force balance in a longitudinal cross section of the in horizontal pipe based on two layered model

Even though some approaches exist for predicting the behaviour of slurry flow (Shook, et al., 2002), Worster and Denny (1955), etc.), the inclination parameter still remains bizarre, and is not explicitly correlated to other flow parameters. That is why this research is an important addition to the existing literature on slurry flows in inclined pipes.

3 Review of existing narrow graded mixture experimental results

This chapter is focused on findings of Matoušek, et al., (2019), “Anomalous pressure drops in settling slurry flow of mild negative slope”, which served as the primary inspiration for my research. In summer of 2018, experiments were carried out at the Institute of Hydrodynamics in Prague, in a 100 mm loop with inclinable inverted U-tube. They consisted of the flow of aqueous mixture with narrow-graded natural sand (fraction code = SP3031), with a mean grain size of 0.55 mm and grain density of 2597 kg/m³. Mean delivered concentration of solids in the pipe was roughly 0.24, which is a common solids concentration in industrial pipes. Tests were carried out in a range of inclination angles from 0 to ± 45 degrees.

3.1 Anomalous pressure drops in descending flow of narrow graded sand-water mixture

In this paper, the authors confirm that there exists a general trend of increasing manometric hydraulic gradient with the increase of inclination angle, which occurs due to the increase in the static part of the gradient. Nevertheless, this trend is interrupted in some cases of negative slopes. Specifically, for negative slopes between -5 to -25 degrees, and with a local peak at -25 degrees. Authors state that this deviation corresponds to those inclination angles where the manometric hydraulic gradient is considerably higher than what the general trend suggests. Moreover, when calculating the frictional gradient, which is obtained by subtracting the C_{vi} -based static part of the manometric gradient, it becomes clear that the anomaly is mostly due to friction gradient.

Later in their paper, the authors also explain this phenomenon in connection with the solids' distribution in the cross-section. Their experimental results show that in horizontal flow, solids have a linear distribution in the pipe cross-section. This condition appears to remain valid in different inclinations of ascending limb (positive angles), but it changes drastically in the descending limb for the above mentioned “critical” angles (negative slopes between -5 to -25 degrees). In these inclinations, the

degree of solids stratification increases significantly and reaches the stratification peak at -15 degrees.

Overall, this paper proved once more (similar findings were published in other journal papers as well, but as I have mentioned in this thesis, still a broader database is needed) that descending flows exhibit more stratification than ascending flows. In ascending flows, the sliding bed moves at a much lower velocity than the flow above it, which produces a high-velocity gradient and therefore the most-top of the sliding bed shears off. This scenario is not present in the descending flows, where the velocity of the sliding bed and of the flow above it, have similar values; thus, the stratification is thicker. In inclination angles steeper than -35 degrees, the conditions change once more; The bed starts to disintegrate since the velocity of solids particles is much higher than that of carrying liquid. All findings are reasonable and can be explained by force balance analysis applied at the two layers of slurry flow.

3.2 Force balance analysis in inclined slurry flow

The slurry flow consists of a carrying liquid and some solids either in motion, in suspension or static state. In many cases, the solids will settle and form a bed, either sliding or stationary at the bottom of the pipe. The pressure gradient forces are the major driving forces in slurry flow. As Matoušek et al., (2019) explain, despite the usual driving and resisting forces present in the flow, a new force is introduced in the inclined flows. The force representing the weight of the submerged solids can be resolved in two components, where one is perpendicular to the longitudinal pipe axis, and the other component is in the direction of the flow. By making a force balance in this situation, the result shows that the submerged solids' weight acts a resisting force in the ascending flow, and on the other hand, as a driving force in the descending flow. This mechanism is clearly visible in the schemes below for both scenarios.

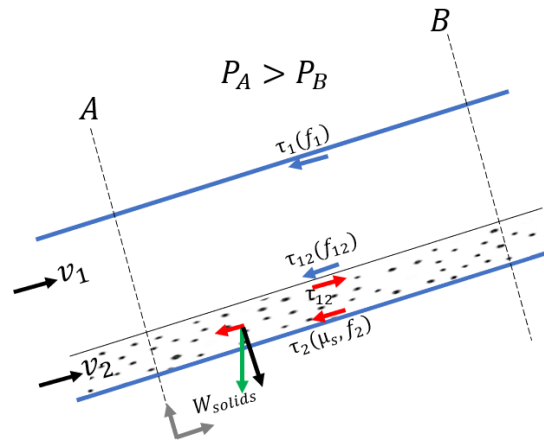


Figure 3. 1 Force balance of slurry flow in ascending pipe based on two layered model

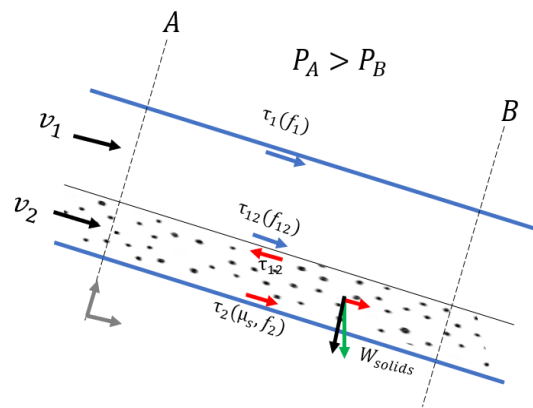


Figure 3. 2 Force balance of slurry flow in descending pipe based on two-layered model

The partially stratified flow has a two-layered structure mostly composed of a sliding bed with a uniform distribution of solids at the bottom and a transport layer.

Coarse settling slurries tend to stratify in both horizontal and inclined section of the pipeline system (Matoušek et al., 2018)

4 Methods

During summer 2019, I was involved in carrying out tests for slurry flow at the Institute of Hydrodynamics (IH) of Czech Academy of Sciences in Prague, in a 100 mm laboratory loop with inclinable inverted U-tube. Amidst the procedure, measurements included mean flow velocity, V_m , by a magnetic flowmeter, manometric pressure drops in ascending and descending limbs of the U-tube, delivered concentration C_{vd} , and chord averaged vertical concentration distribution by gamma-ray radiometric profilers mounted to the pressure-drop measuring sections of both limbs of the U-tube. Similar experiments with broadly graded slurry were conducted in a 203 mm pipeline in the GIW Hydraulic Lab (Visintainer, et. al., 2017), which even served as a guideline to me.

4.1 Experimental facility

The laboratory loop consists of steel pipes with a diameter of 100 mm, and it includes a U-tube section which can be inclined to angles ranging from -90 to + 90 degrees. The loop also consists of some clear sections, made of plexiglass, and they are used for visual observation of the flow inside the pipe. Such sections are present in all three cases: horizontal, ascending, and descending section. The flow parameters are measured simultaneously in the ascending and descending pipes thanks to the U-tube presence. These measurements include solids distribution across the pipe cross-section, manometric pressure differences, average velocity in the pipe and delivered concentration of solids C_{vd} .

Solids distribution in a cross-section is one of the most important features of the flow. It is measured using the method of gamma radiation absorption of a radiometric instrument. The instrument is a radiometric density meter, which moves along the pipe circumference and consists of a radiation source and a detector (it is usually very safe due to multiple coverages). The radiative power exists the Gamma-ray source ($^{137}\text{Caesium}$ in this case) on one side of the pipe, and after some internal process, a stochastic signal is produced from the detector on the opposite side. This signal is further processed from an electronic system. Since the radiation is weakened when penetrating some matter, it is possible to measure the solids concentration on signal intensity change basis. The radiometric density meters are located near the clear sections in both legs of the U-tube in the laboratory loop. Having them in this position,

it is possible to make an evaluation of the situation by a trained-eye and thus make a practical accuracy check of the instrument itself.

The pressure losses are calculated by manometric pressure differences throughout the pipe. In the laboratory loop at the Hydrodynamic Institute, six differential pressure transmitters (DPT) are located along the entire loop, including both legs of the U-tube.

The average velocity of the flow is measured by a magnetic flow meter in the vertical section of the loop.

4.2 Tested mixture specifications

Selection of the mixture components was made based on previous experimental data (Matoušek et al., 2019) obtained at the same facility. In 2018, tests were carried out with an aqueous-sand mixture, consisting of a narrow-graded medium-sized natural sand with mean particle size $d_{50} = 0.55\text{mm}$ (fraction code = SP3031).

New tests were carried out with a broadly graded natural sand of the same d_{50} as the narrow graded. The mixture consisted of three narrow graded sand fractions: coarse sand (fraction code = SP0612), medium sand (fraction code = SP3031) and fine-graded (fraction code = STJ25 ~ Strelec). To obtain the same d_{50} , proportions of each individual fraction were calculated in advance.

	Particle size range [mm]	d_{50} [mm]	Ratio in mixture
SP0612	0.25 - 2.00	1.00	38%
SP3031	0.10 - 1.50	0.55	31%
STJ25	0.125 - 0.40	0.275	31%

Table 4. 1 Sand particle analysis

The table above is the result of particle analysis for each of the fractions, which I made after the sieve testing. Dry sieve testing was performed in laboratory conditions. Following the standard procedure for sieve testing (Craig, 2014), different sieve sizes were put one above the other, and then the sample of interest was poured into the stack. A sieve shaker was used for shaking all the sand particles, in order to get accurate results. The same procedure was followed for the mixture as well.

Afterwards, raw data were uploaded in an excel file, which was prepared for calculating the cumulative passing percentage for each sieve size. The PSD curve is a

semilogarithmic scale, where the particle diameter is logarithmic, for the purposes of statistics (Garcia, 2013). A semilogarithmic plot produces readable results, which makes it easier to get a similarity check between any two PSD curves of different samples. To obtain a smoother transition though measured points, some interpolation was required for the sieve sizes that were missing in the raw data.

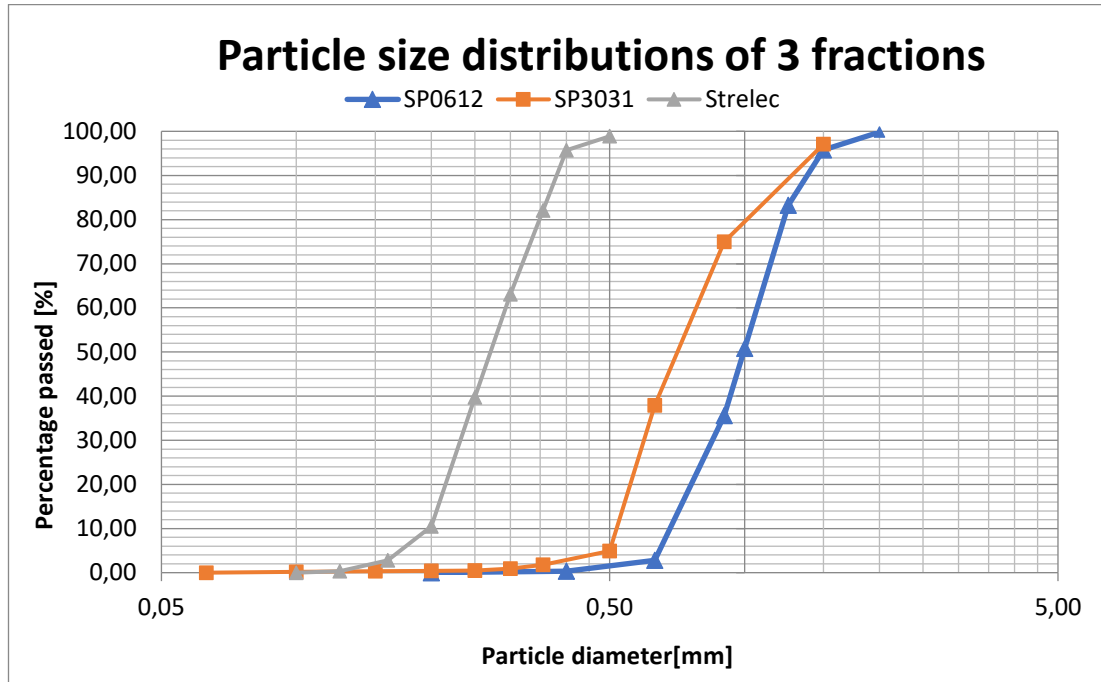


Figure 4. 1 Particle size distribution curve of three narrow graded sand samples, which compose the broadly graded sand

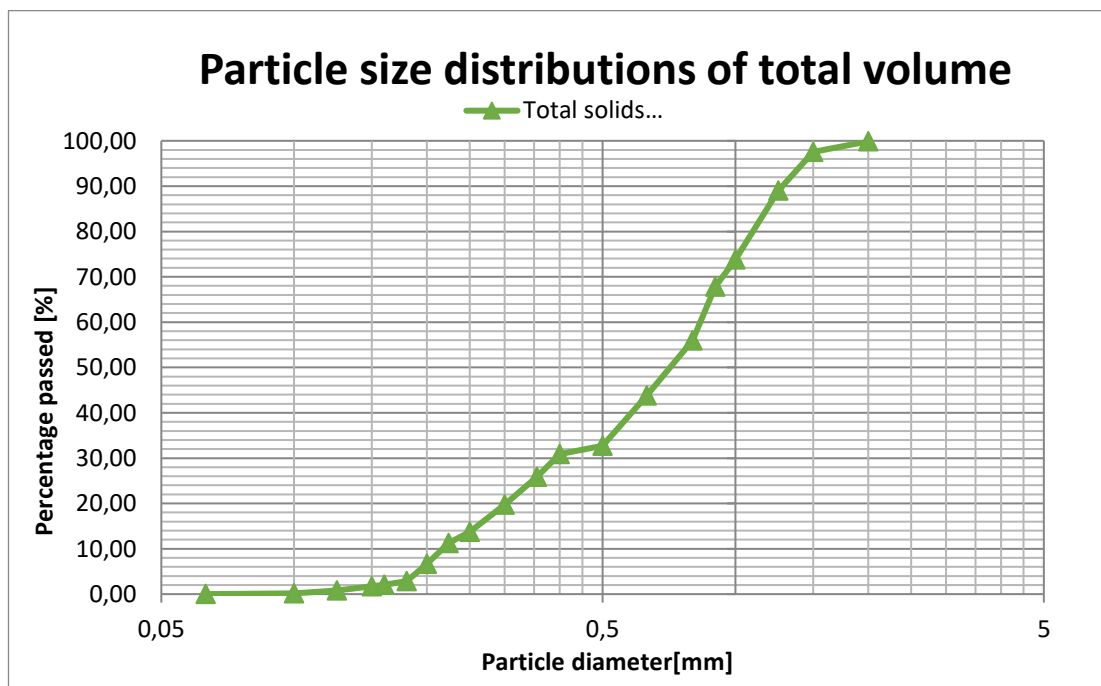


Figure 4. 2 Particle size distribution curve of broadly graded sand (fraction code = S063025)

Particle size distribution curve of broadly graded sand is much smoother than the medium fraction of narrow graded sand.

4.3 Analysis of the data

Data processing is a key mechanism in data analysis and modelling, and it consists of a series of steps, depending upon the need of processing length. The raw data are usually processed through a computer software or in specific cases, a code is implemented to accept raw data and provide outputs. In the IH Prague, a unique software is used to pre-process the data that are collected from the laboratory loop measurements and these data are then stored in text files, in proper formatting, which can be easily used in several existing/new codes. The text files derived from the software are still unable to provide significant information to the user, therefore further processing is necessary. Some preparation of text files and the receiving code is necessary for successful import of the data into the code/model of interest. In the case of slurry flow measurement at IH Prague, this step was then followed by using MATLAB software, which is a strong modelling tool for researchers, to make use of the data. The pre-processed data are called into the adequate files and are used as part of models to make calculations, plotting, and give final results, which we call the output.

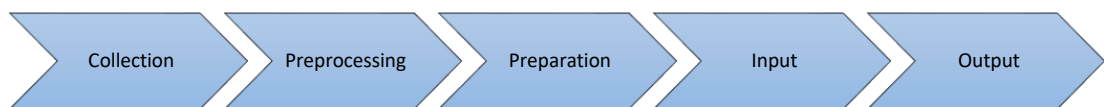


Figure 4. 3 Data processing steps

5 Results and discussion of experimental results

It is generally accepted that broadly graded slurries exhibit less friction than narrow-graded slurries. However, there are only a few experimental data to prove that in inclined flows. Previous experiments have revealed that flows consisting of coarse material only, create the pattern of a granular bed sliding at the bottom of the pipe. Late research conducted in the GIW Hydraulic laboratory, focused on slurry flow with a combination of four different fractions, each representing one type of settling slurry (carried-fluid fraction ~ fine, pseudo-homogenous fraction, heterogenous fraction, stratified fraction ~ coarse), showed that mixing of particle sizes has an impact in the slurry behaviour. As I have mentioned several times in this thesis, the most important aim of this research is to determine the effect of particle size grading to the behaviour of inclined flows, especially on the hydraulic gradient (both frictional and manometric), and solids distribution within the pipe. Below, I will present the results of my experiments, and furthermore discuss the findings.

5.1 Solids concentration in the pipe

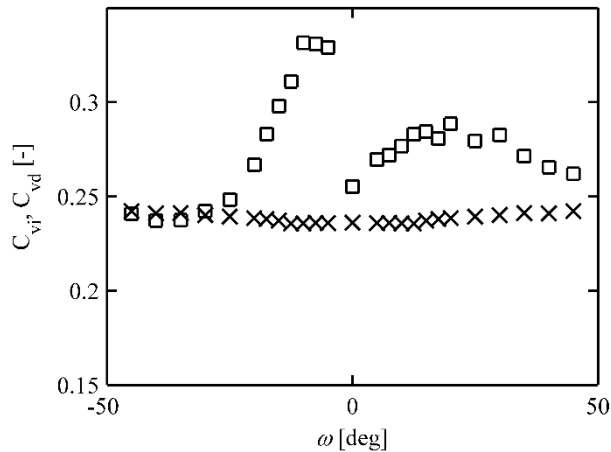


Figure 5. 1 Experimentally determined volumetric concentrations of solids in sand-water flow at $V_m \approx 2.5$ m/s and $C_{vd} \approx 0.24$ at different inclination angles. Legend: square marker: Spatial volumetric concentration C_{vi} ; x-marker: Delivered volumetric concentration C_{vd} .

The figure above shows the spatial and delivered concentration of solids in various flow inclination angles. Plotting the two together allows the comparison and quantification of their differences. In horizontal flow and flow of mild positive/negative inclination angles, the difference between C_{vd} and C_{vi} is non-negligible. The highest contrast is detected in descending flows, where the spatial

volumetric concentration can reach about 20% higher values than the delivered concentration in mild slopes, which indicates that the solid particles are moving slower than the carrying liquid. In the flow of inclination angles -40 and -35 degrees, C_{vi} reaches slightly lower values than C_{vd} showing that the solid particles are moving faster than the carrying liquid. On the other hand, the difference between delivered and spatial concentration values tends to reach zero in steeper positive inclinations, displaying that the phase slip is negligible at those angles.

The ratio of solids used in this experiment is commonly used in industries. However, the necessity to make the operation of pipelines more efficient is requiring a higher proportion of solids to be transported. This advancement carries the risk of total stoppage of the solids' volume and clogging the section of pipeline which runs in these mild inclination angles. This issue should be considered in the design process of a pipeline with similar parameters.

5.2 Concentration profiles

In the plots in Figure 5., we can see the development of concentration profiles at a mean pipe velocity of 2.5 m/s. Concentration profiles presented here belong to the following range of inclination angles: 0 , ± 5 , ± 10 , ± 15 , ± 20 , ± 25 , ± 35 , ± 45 degrees. The first plot shows that the horizontal flow has no significant stratification in both measuring sections of the U-tube set at horizontal position. The solids distribution is almost linear in the entire cross-section at 0 degrees. This condition changes slightly in inclined ascending flows, where none to very thin sliding bed is present. On the contrast, the solids distribution in the descending limb of the pipeline shows a very different picture. Flow in almost all negative slopes is stratified to some degree, and when inclined to angles say -10 to -20 degrees, a full sliding bed is present.

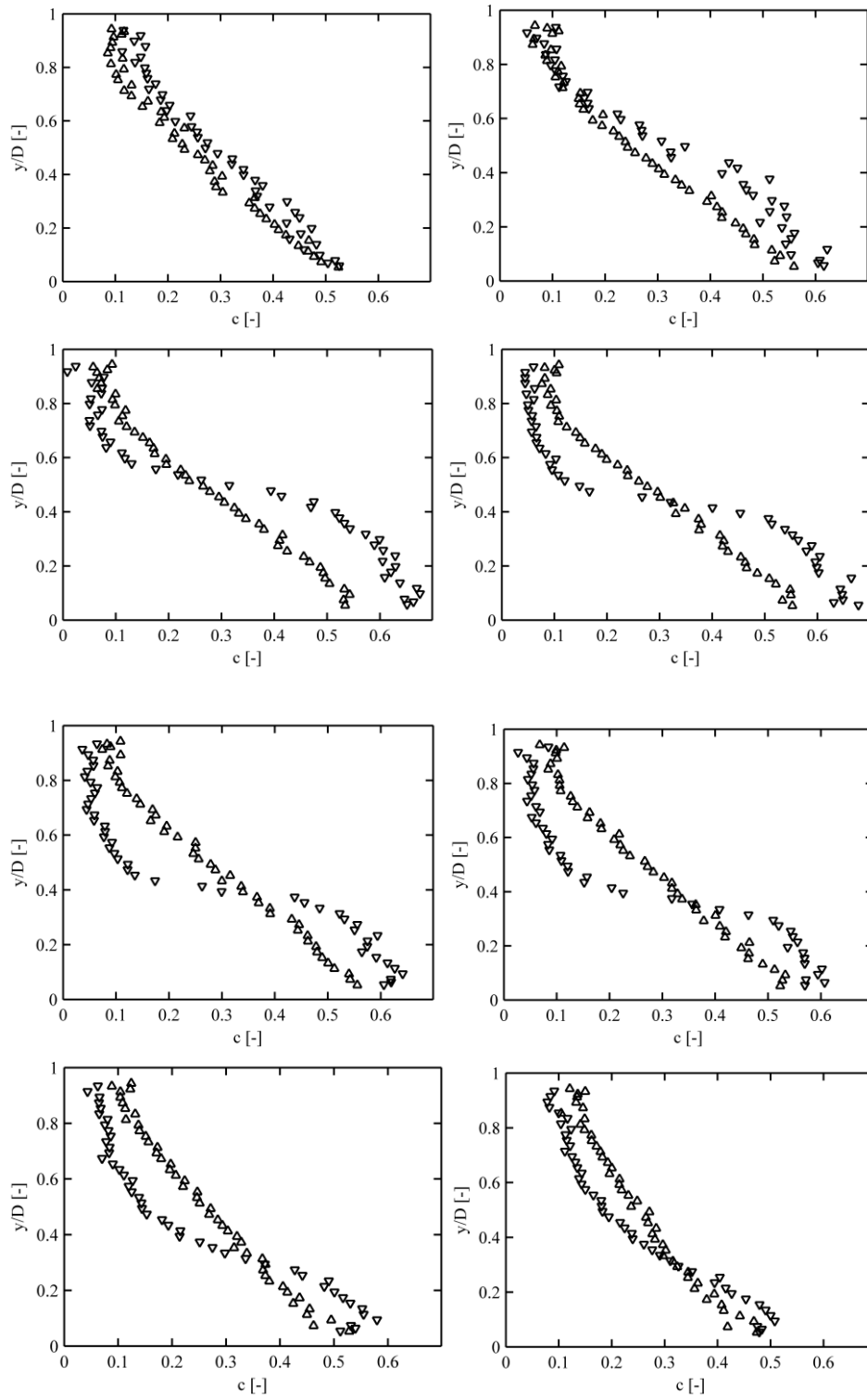


Figure 5.2 Measured solids distributions in broadly graded sand-water flow at $V_m \approx 2.5$ m/s and $C_{vd} \approx 0.24$ at inclination angles from 0 degree (upper-left plot) to ± 45 degrees (down-right plot). Legend: red o-line: narrow graded sand-water test; blue d-line: broadly graded sand-water test

A thick sliding bed was also visually realized through the transparent section in the pipe. Inclinations steeper than -25 degrees show a reduction of the thickness of sliding bed, which can be related to the differences of volumetric concentration in these slopes and indicate that the solids' bed at the bottom of the pipe slides faster than the carrying liquid. An exciting outcome of the experiments was visualizing the layering of solid particles in the sliding bed. While the coarse particles travel through the pipe as a sliding bed, a considerable amount of finer particles are trapped at the bottom layer, travelling together or not. However, some part of very fine particles continues to be in suspension during the flow, creating the 'heavy medium', and some may not settle even long after going back to no-flow condition (this is shown in the figure below, where the carrying liquid looks dirty because of these very fine particles in it).



Figure 5. 3 Layering of particles at the bottom of the pipe, clear horizontal section; no flow condition. Overall, the effect of inclination in the particles' distribution in the pipe is significant. The change is considerably higher in negative slopes, where the flow is fully stratified.

5.3 Hydraulic pressure gradient

Estimation of pressure drops in the pipeline is a crucial design parameter and a major objective of this thesis. Along with the static pressure gradient, which results in cases of potential energy change, the frictional gradient is of high importance for further calculations. Several correlations exist for predicting the friction factor and the total friction losses, but yet, most of them are of an empirical nature. In this section, I will present the measured pressure losses in my experiment, as an attempt to broaden the available database for further research.

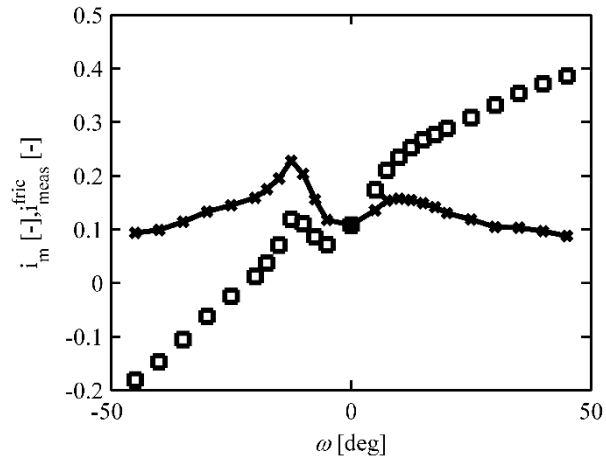


Figure 5. 4 Different hydraulic gradients (dimensionless pressure drop) in sand-water flow at $V_m \approx 2.5$ m/s and $C_{vd} \approx 0.24$ at different inclination angles. Legend: black square marker: measured manometric gradient; black x-line: frictional gradient from measurements

Experimental results show that pressure gradients are sensitive to the inclination angle. A general increase of manometric pressure gradient with the increasing inclination is determined, and it is attributed to the effect of the static part of the gradient. This trend though is interrupted in mild negative inclinations, as the friction gradient reaches higher values than anticipated. The unusual pressure drop reaches a local peak at -15 degrees, and it corresponds to the allocation of C_{vi} peak and the stratification thickness. Pressure drop anomaly occurs due to a change of phase-slip condition and a varying frictional gradient in different inclinations in the pipe. The correlation of frictional pressure drop and solids distribution is logically determined by force balance analysis, which gives a clear understanding of the underlying mechanism (it was explained in Chapter 3).

6 Comparison of broadly graded and narrow graded sand-water flow

The conducted experiments have produced a database for broadly graded slurry, directly comparable to narrow graded slurry.

In the mean pipe velocity comparison plot, a smooth line for the broadly graded slurry is observed. While conducting the experiment, the mean velocity in the pipe was kept at about 2.5 m/s, which was easy to be achieved in more stable condition in the broadly graded slurry. In the narrow-graded slurry experiment, the flow was less stable, so there are also slight fluctuations in mean velocity as well. The flow is more sensitive to the inclination angle change for narrow-graded, compared to broadly graded slurry.

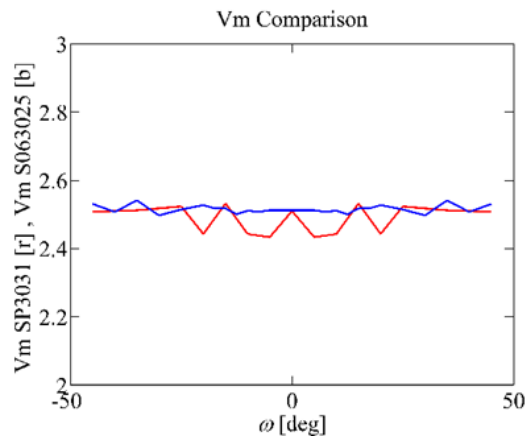


Figure 6. 1 Mean velocity in the pipe comparison; Legend: b-line: broadly graded; r-line: narrow graded

Concentration of compacted sand in mixture with water for two cases:

Broadly graded: 64.9% Narrow graded: 63.0%.

A comparison of narrow graded and broadly graded slurry flow show that solids' distribution in the pipe cross section is sensitive to the inclination in both cases. In the horizontal flow, we observe a similar behavior of the flow for both cases. The flow is heterogenous, not stratified, and solids are almost linearly distributed in the cross section.

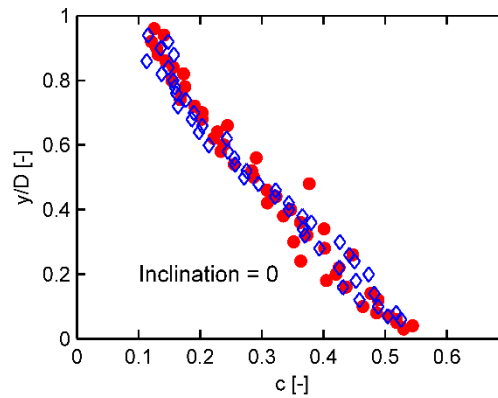


Figure 6. 2 Measured solids distributions in sand-water flow at $V_m \approx 2.5$ m/s and $C_{vd} \approx 0.24$ at horizontal flow. Legend: red circle: narrow graded sand-water test; blue diamond: broadly graded sand-water test

In the ascending slurry flow, i.e. positive inclination angles, we observe a similar shape of concentration profiles. No to minimal stratification is present in the slurry flow with broadly graded sand particles, while there is a slight stratification visible in the flow of narrow graded slurry. This slight change supports the previous statement by showing how sensitive the flow resistance is to the particle distribution. This mechanism explains the correlation of the solids' effect with solids' distribution in the pipe. It shows that where more stratification is present, the hydraulic gradient is higher and the other way around. Following the aftermath of this mechanism, it is clear that a slurry flow with broadly graded particles is more efficient due to fewer frictional head losses.

In the descending slurry flow, i.e. negative slopes, more significant changes are observed in the shape of concentration profiles for narrow and broadly graded slurries. Contrary to positive inclinations, in the negative slopes, there is a significant thickness of the sliding bed present in the flow in both cases. Following the development of the concentration profiles, it is observed that the flow tends to stratify in less steep inclinations in the narrow-graded slurry, and the same conditions remain for a more extensive range of inclinations compared to the broadly graded slurry. This observation emphasizes that pipelines carrying narrow graded slurries have more limitations in their design.

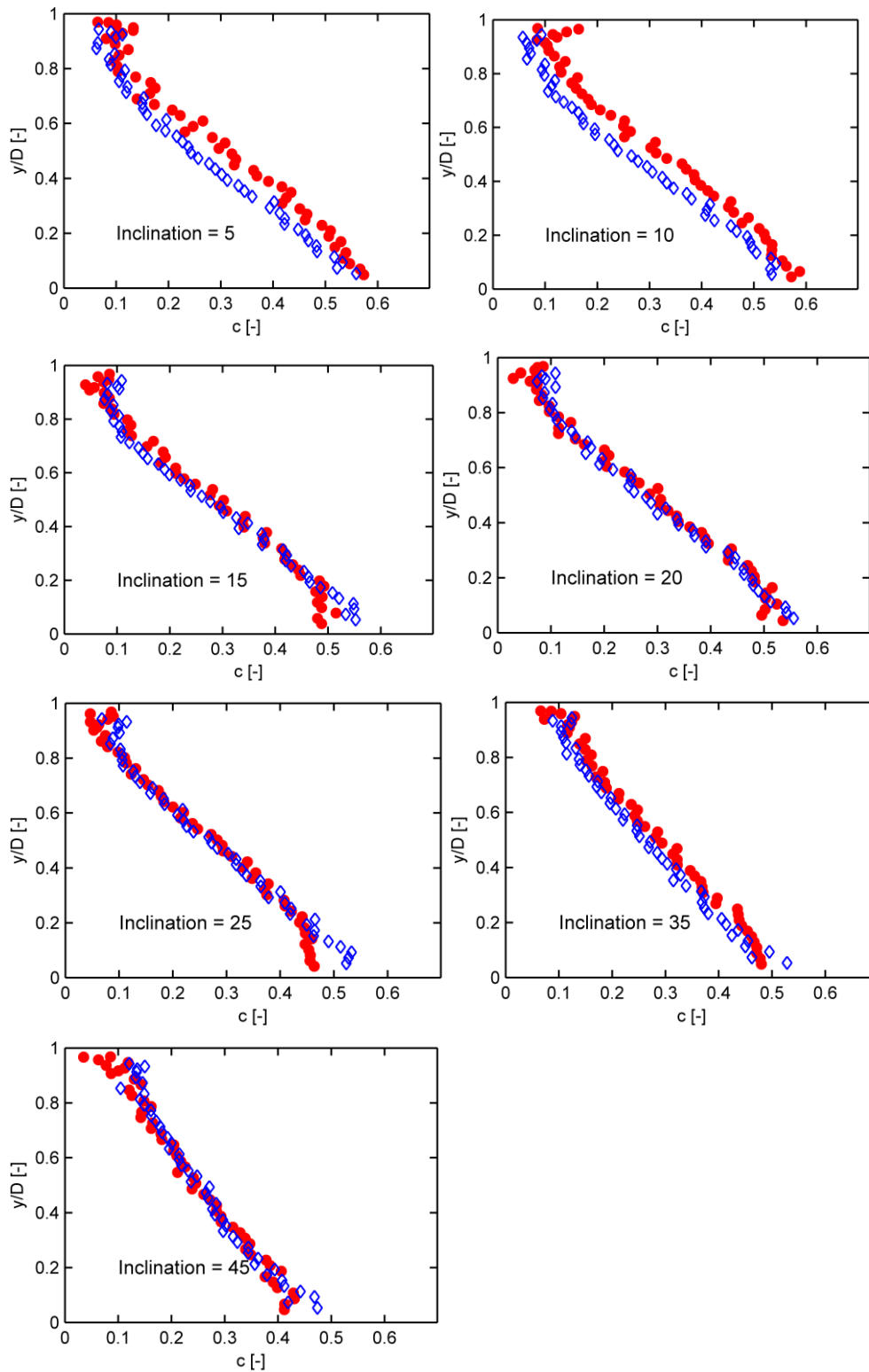


Figure 6. 3 Measured solids distributions in sand-water flow at $V_m \approx 2.5$ m/s and $C_{vd} \approx 0.24$ at positive inclination angles. Legend: red circle: narrow graded sand-water test; blue diamond: broadly graded sand-water test

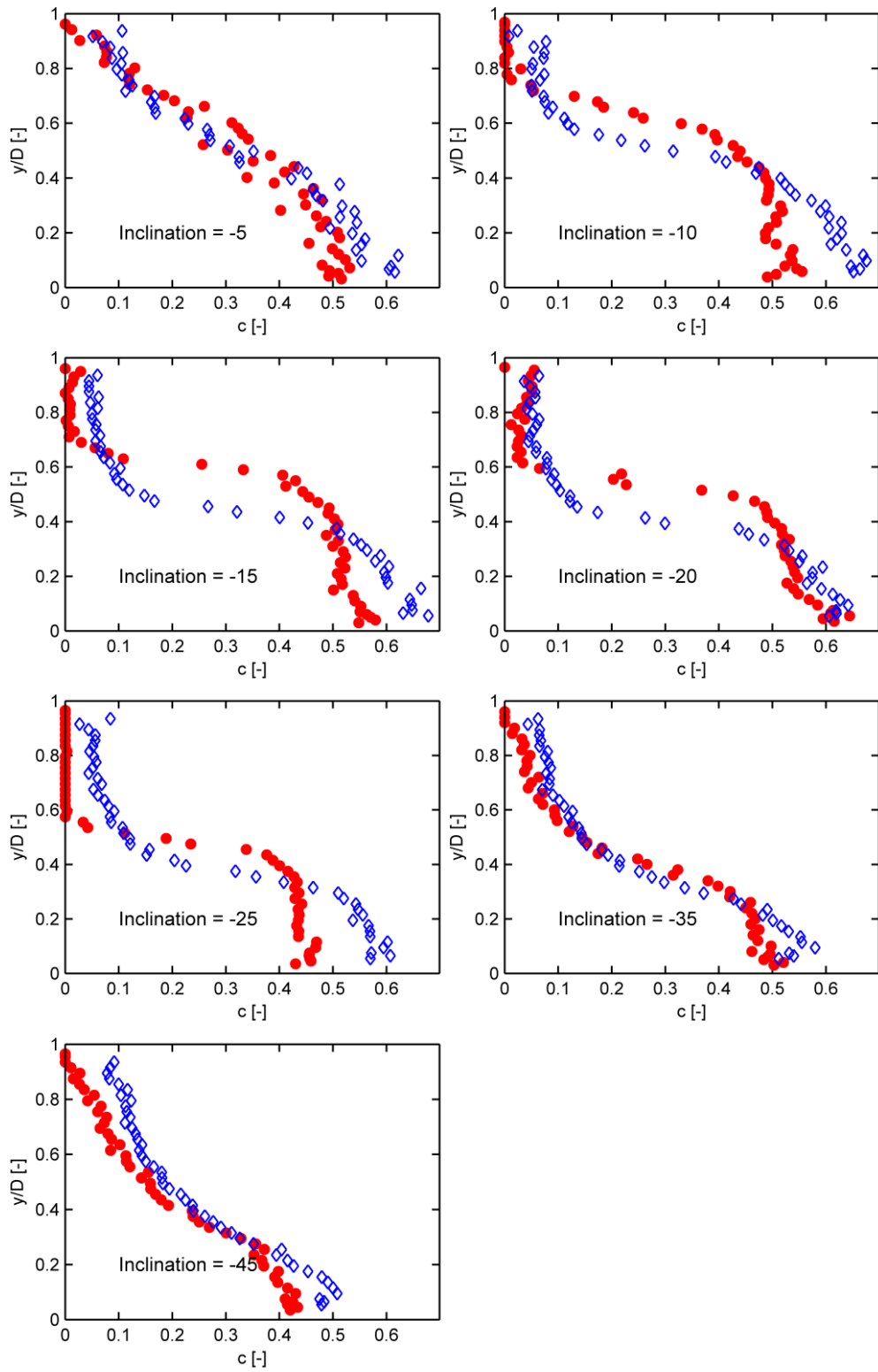


Figure 6. 4 Measured solids distributions in sand-water flow at $V_m \approx 2.5$ m/s and $C_{vd} \approx 0.24$ at negative inclination angles from -5 to -45 degrees. Legend: red circle: narrow graded sand-water test; blue diamond: broadly graded sand-water test

From the experimental results, the trend of a thick sliding bed in the narrow-graded slurries and a thin sliding bed for the broadly graded slurries is observed. The proportion of solids to water in the slurry remains similar though, and that difference is adjusted by higher values of concentrations in the broadly graded slurry. i.e. broadly graded slurry flows are characterized by a thin, highly concentrated sliding bed, while narrow graded slurry flows are characterized by a thick, relatively less concentrated sliding bed. There is less amount of particles in suspension in the flow of narrow graded slurry, while in the broadly graded slurry, the finest particles almost never settle, so there is always some amount of particles in the flow above the sliding bed. The sliding bed is sharply defined in the narrow-graded slurry flow, which comes as a result of the slip between two layers. In the broadly graded slurry flow, the bed stratification is more linear, due to the vast range of particle sizes; while the coarse particles settle at the bottom of the pipe, some finer particles either fill the pores created at the bed or are moving in suspension just above the lower layer.

These observations support the mechanism explained in the literature (Matoušek, et al. 2019). In the slopes between -10 and -35 degrees, the most significant difference in the shape of concentration profile is detected, where the narrow-graded slurry is fully stratified, and in these observation points we also have the biggest difference of the frictional pressure losses.

6.1 Anomalous element in the concentration profiles

One interesting occurrence visible in the concentration profiles is the concentration peak, which sometimes is not exactly in the very bottom of the pipe. So, based on our measurements, there can be detected a higher solids concentration slightly above the pipe surface, compared to the concentration at the pipe surface. This phenomenon can be explained firstly by possible uncertainties in our measurements. This experiment is carried out using two radiometric devices to determine the solids concentration in the pipe. There is a possibility that the radiometric device behaves abnormally near the pipe surface which is later reflected in these results.

In another scenario, this could be explained by the solids' interaction. In the bottom of the pipe, there is a sliding bed which consists of sand particles. These sand particles interact with each other by means of collisions, which subsequently bring up the

suspension mechanism. In the case that particles tend to suspend other particles in the bottom of this sliding bed, we can be faced to a very bottom layer of particles with a particular concentration, and the next layer above that, where the adjacent particles are suspended, with a slightly higher concentration. This idea is supported by the fact that this phenomenon is more visible in flows of steeper angles, both positive and negative (but mostly negative), where the collision of particles with each other is prominent.

7 Modelling slurry flow

7.1 Worster-Denny prediction of frictional pressure losses

As the Worster-Denny formula is widely used in predicting pressure losses in the pipe, both manometric and frictional, and it takes into consideration the inclination effect, I made test runs with the newly produced data of broadly graded sand-water slurry. Of course, the formula accounts just one mean size of the particles (in this case $d_{50} = 0.55$ mm) and produces same results on both direction of the limb, so no accurate prediction is expected.

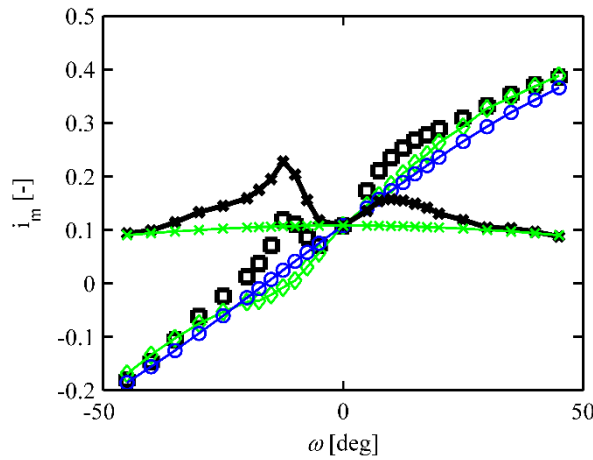


Figure 7. 1 Different hydraulic gradients (dimensionless pressure drop) in sand-water flow at $V_m \approx 2.5$ m/s and $C_{vd} \approx 0.24$ at different inclination angles. Legend: black square marker: measured manometric gradient; black x-line: frictional gradient from measurements; blue o-line: manometric pressure gradient from Worster-Denny formula based on C_{vd} ; green diamond-line: manometric pressure gradient from Worster-Denny formula based on C_{vi} ; green x-line: frictional gradient by Worster-Denny based on C_{vi}

Modelling pressure losses in inclined slurry flow of broadly graded material using the Worster-Denny formula, does not give very accurate results, as was assumed. Worster-Denny approach to estimate pressure gradients is able to produce reliable results for horizontal flow, however, it underestimates the high pressure drops which occur especially in mild inclination angles, both positive and negative. The error of the predicted values is higher for descending flows, since Worster-Denny formula calculates the inclination effect symmetrically, i.e. both positive and negative inclinations exhibit same friction gradient, while in reality, the descending flows exhibit more friction. Usage of spatial volumetric concentration C_{vi} instead of delivered volumetric concentration C_{vd} improves the performance of the model

slightly, but the change is not significant. The formula's efficiency increases for flows steeper than ± 35 degrees.

7.1.1 Empirical modification of Worster-Denny formula for friction gradient

There exists a significant analogy between the frictional hydraulic gradient plot and the spatial concentration plot. Therefore, my hypothesis is that the friction gradient is dependent on the C_{vi} , and C_{vi} should be included in its calculation.

Below I will present the results of some attempts to modify the Worster-Denny formula for prediction of friction gradient in inclined flows of broadly graded material, based on the retrieved experimental results.

Original Worster-Denny:

$$(i_m^{\text{fric}} - i_f) = (i_{m,0}^{\text{fric}} - i_f) \cos \omega \quad (12)$$

Attempt 1:

$$(i_m^{\text{fric}} - i_f) = (i_{m,0}^{\text{fric}} - i_f) \cos \omega + (C_{vi} - C_{vd}) \quad (13)$$

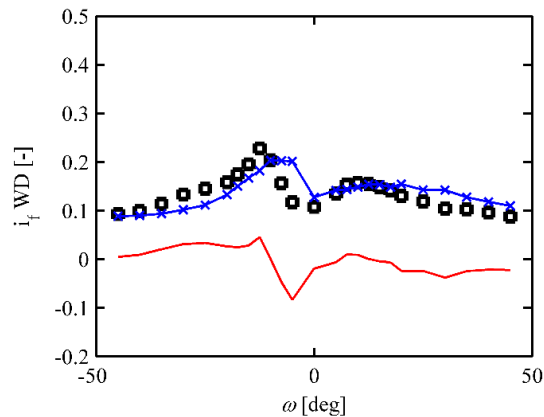


Figure 7. 2 Modification of Worster-Denny formula to predict friction losses. Legend: black square marker: measured friction gradient; blue x-line: frictional gradient from modified Worster-Denny; red-line: error between measured and calculated friction gradient.

The resemblance of C_{vi} trend and the friction gradient is very clear, therefore it is necessary to include this concentration parameter in the equation. This attempt introduces in the equation the difference between the spatial volumetric concentration and delivered volumetric concentration, which employs in the results only the

anomalous shape which is present both in the friction gradient and the spatial volumetric concentration.

Attempt 2:

$$(i_m^{\text{fric}} - i_{m,0}^{\text{fric}}) = C_{v_i}(S_s - S_f) \cos \omega \quad (14)$$

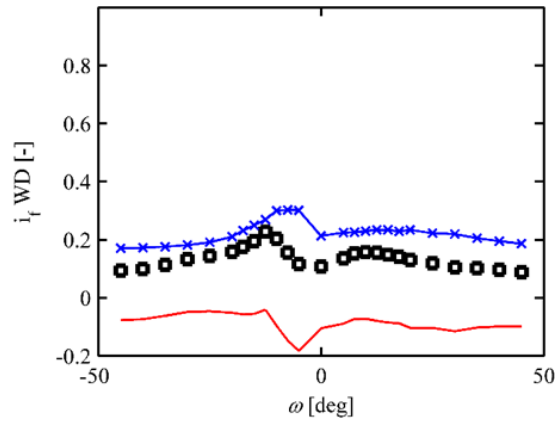


Figure 7. 3 Modification of Worster-Denny formula to predict friction losses. Legend: black square marker: measured friction gradient; blue x-line: frictional gradient from modified Worster-Denny; red-line: error between measured and calculated friction gradient.

Attempt 3:

$$(i_m^{\text{fric}}) = C_{v_i}(S_s - S_f) \cos \omega \quad (15)$$

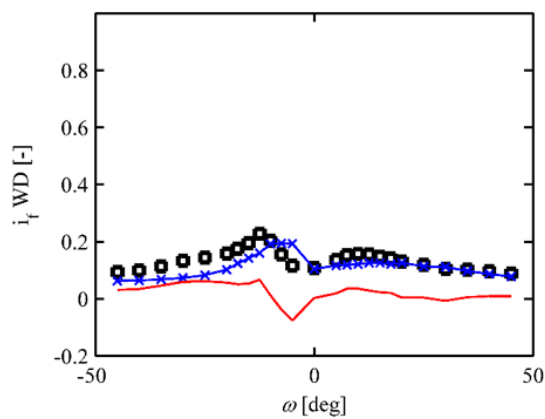


Figure 7. 4 Modification of Worster-Denny formula to predict friction losses. Legend: black square marker: measured friction gradient; blue x-line: frictional gradient from modified Worster-Denny; red-line: error between measured and calculated friction gradient.

7.2 Two-layered model

Even though several models exist for predicting the behaviour of slurry flow (Shook, et al., 2002), Worster and Denny (1955), etc.), the inclination parameter still remains bizarre, and is not explicitly correlated to other flow parameters. The two-layered model of Matoušek (2009), which I refer to in this thesis, considers two layers with an interfacial sub-layer, called shear layer, embedded in the upper layer and, and was lately upgraded to predict also inclined slurry flow parameters. Different from other two-layered models, Matoušek (2009) and Matoušek and Krupička (2014), developed a model where the delivered volumetric concentration is an input and the spatial volumetric concentration is an output (Miedema, et. al., 2016)

This model is calibrated to work with raw data that are received from the experimental laboratory tests and is able to produce satisfying results for different pressure gradients, different volumetric concentrations, and concentration profiles. The input and output parameters of the model are listed below.

Input

The two layered model has several input parameters:

- Geometry [m] consisting of the size of the pipe, circular or rectangular;
- V_m [m/s] mean velocity of the flow;
- C [-] concentration of solids, delivered or volumetric;
- C_{mode} [1/2] which defines the type of concentration input;
- d_{50} [m] particle size diameter;
- Ro_s [kg/m^3] solid particle density;
- Ro_f [kg/m^3] fluid density;
- ν_f [m^2/s] fluid kinematic viscosity;
- C_{b0} [-] concentration in stationary bed;
- $C_{b_{lim}}$ [-] concentration in sliding bed;
- V_{2lim} [-] threshold velocity of bed for $C_{b_{lim}}$;
- V_t [m/s] particle settling velocity;
- k_w [m] pipe wall roughness;
- m_i [-] wall/contact load friction coefficient;
- f_i [rad] dynamic friction angle of solids;

- K [-] coefficient of mud pressure;
- omegaDeg [deg] pipe inclination angle;
- fricEq [integer] represents the friction equation linked to a number;
- transpEq [integer] represents the transport equation linked to a number.

Output

Outputs of the model are (Matoušek, et. al., 2018):

- the total pressure drop;
- the frictional component on the total pressure drop;
- the thickness of the contact layer;
- the distribution of the solids above the contact layer;
- the average velocity of the contact layers V_2 , and of the upper layer V_1 ;
- the average solids concentration in the upper layer, C_{v1} ,
- the solids concentration (either C_{vi} or C_{vd} , the one which is not an input, according to the selected mode).

7.2.1 The fundamental equations

This two-layered model is capable of predicting flow parameters using different existing equations from the literature. The most important equations describing the slurry flow are the transport equation and the friction equation, which can be added or changed in the model, and are identified with an integer of choice. Therefore, in the of validating this model for the broadly graded slurry mixture, I have tested some existing friction and transport equations, from the literature, which are suitable for the current data. There is a range of empirical equations to compute the friction parameter of the interface, while the model counts on the transport equation of Matoušek (2009), or Matoušek and Krupička (2014), since it has proved to be effective in all the previous research. The current version of the model is tested for the inclined, narrow graded slurry flow using the following friction and transport equations.

Transport of solids

In the previous studies, the authors suggested the MPM-type of transport equation, in two different forms:

1. Matoušek (2009)
2. Matoušek (2009), modified Krupička, (2014).

The transport of solids above the contact layer, in both cases, is determined by using the Meyer-Peter and Müller formula type (US Soil Conservation Service, 1983). The used version of MPM formula has been obtained by integrating a product of local velocities and concentrations of solids over the discharge area of a shear layer, and has been calibrated by a large number of experimental data for horizontal flows (Matoušek and Krupička, 2014):

$$\Phi = \left(\frac{3.13}{0.6} + \frac{C1}{Re_p^{0.62}} \right) * \theta^{\left(1.2 + \frac{C2}{Re_p^{0.39}} \right)} \quad (16)$$

where the Einstein transport parameter:

$$\Phi = \frac{q_s}{\sqrt{\frac{(\rho_s - \rho_f)}{\rho_f * g * \cos\omega * d_{50}^3}}} \quad (17)$$

the sediment volumetric discharge per unit width of bed:

$$q_s = \frac{C_{v1} * A_1 * (V_1 - V_2)}{O_b} \quad (18)$$

and the particle Reynolds number:

$$Re_p = w_t * \cos\omega * \frac{d_{50}}{\nu_f} \quad (19)$$

The values of C1 and C2 were initially estimated as C1= 58 and C2=1.3 in Matoušek (2009) and recalibrated by Krupička (2014) as C1= 39 and C2=2.6, using a large database that includes different pipes and solids fractions. Both versions of this transport equation are valid and can be used in different circumstances.

Interfacial friction

A log law is used to formulate a friction equation for an eroded granular bed. The log law relates the friction coefficient λ_{12} with the hydraulic radius of discharge area associated with the top of the contact layer R_{h12} and the equivalent roughness of the top of the bed k_s .

$$\sqrt{\frac{8}{\lambda_{12}}} = \frac{1}{\kappa} * \ln \left(\frac{B_s * R_{h12}}{\kappa_s} \right) \quad (20)$$

where κ is the von Karman constant (typically 0.4) and $B_s = 14.8$ is a constant for pressurized pipe flows. Matoušek and Krupička (2014) suggested this formula:

$$\kappa_s = d_{50} * 1.35 * W_{s*}^{0.5} * \theta^{1.58} \quad (21)$$

where W_{s*} is the dimensionless grain parameter;

$$W_{s*} = \sqrt[3]{\frac{(\rho_s - \rho_f)}{\rho_f g * \cos \omega}} * w_t * \cos \omega \quad (22)$$

w_t is the terminal settling velocity of solids, and θ is the interfacial Shields parameter.

$$\theta = \frac{\tau_{12}}{\sqrt{(\rho_s - \rho_f) * g * \cos \omega * d_{50}}} \quad (23)$$

Regarding the interfacial friction, the log law for the hydraulically rough boundary is used (as described in the previous paragraphs), with k_s representing the roughness height of the top of the bed. There still seems to be a need for a bed friction formula which is simple and general enough, therefore, this parameter, k_s , is my subject of study, as it is highly sensitive to different slurry flow characteristics.

I have tested a number of existing equations describing the roughness coefficient, k_s :

1. $k_s = 260 * \frac{A1}{01+012} * \left(\frac{V_t \cos \omega}{DV} \right)^{2.5} * |\theta|$ (Matousek and Krupička, 2008)
2. $k_s = d_{50} * 1.3 * |\theta|^{1.65}$ (Matousek, 2003)
3. $k_s = d_{50} * 3.3 * |\theta|$ (Wilson and Pugh, 1988)

$$4. k_s = d_{50} * (2 + 0.6 * |\theta|^{2.5}) \quad (\text{Sumer et al., 1996})$$

$$\text{or } k_s = d_{50} * \left(4.5 + \frac{1}{8} e^{0.6 * \left(\frac{V_t \cos \omega}{u_{\text{shear}}} \right)^4 * |\theta|^2} * |\theta|^{2.5} \right)$$

$$5. k_s = \left(1.7 * WS_*^{1.1} * (g * \cos \omega)^{1.15} * DV^{-2.3} * d_{50}^{0.68} * |\theta|^{1.4} * \right.$$

$$\left. \left(\frac{1}{14.8} e^{\frac{0.4 * |DV|}{u_{\text{shear}}}} \right)^{1.47} \right)^{\frac{1}{0.47}}$$

(Matousek and Krupička, 2010)

$$6. k_s = d_{50} * 3.30 * |\theta|^{1.43} \quad (\text{Krupička, 2014})$$

$$7. k_s = \left(6 * WS_*^{0.83} * (g * \cos \omega)^{0.955} * |DV|^{-1.91} * d_{50} * |\theta|^{1.52} * \right.$$

$$\left. \left(\frac{1}{14.8} e^{\frac{0.4 * DV}{u_{\text{shear}}}} \right)^{0.955} \right)^{\frac{1}{0.005}} ;$$

(Simplified Camenen, et. al.,

(2006), recalibrated Krupička (2014))

$$8. k_s = d_{50} * \left(0.6 * 1.8 * \frac{WS_*^{1.2}}{Fr^{2.4}} * |\theta|^{1.7} \right) \quad (\text{Camenen, et. al., 2006})$$

$$9. k_s = d_{50} * (1.35 * WS_*^{0.5} * |\theta|^{1.58}) \quad (\text{Shields and } V_t^* \text{ calibrated on the IH Prague data only})$$

$$10. k_s = 2 * d_{50} \quad (\text{Yalin, 1992})$$

$$\text{where, } WS_* = \sqrt[3]{\frac{\left(\frac{\rho_s - 1}{\rho_f} \right)^2}{g * \cos \omega * v_f}} * W_t * \cos \omega .$$

The results of all the tests are presented in the next sections.

7.2.2 Original results of the IILM for prediction of inclined broadly graded slurry flow behaviour

For the prediction of inclined slurry flow with broadly graded sand I tested and used the two-layered model from Matoušek, et. al., (2018). As mentioned above, this model was updated to take into account also the inclination angle, therefore it is suitable to be used with my experimental data. I have run the model using the existing parameters as for the friction ($\text{frictEq} = 9$) and transport formula ($\text{transpEq} = 2$) and the results are presented below.

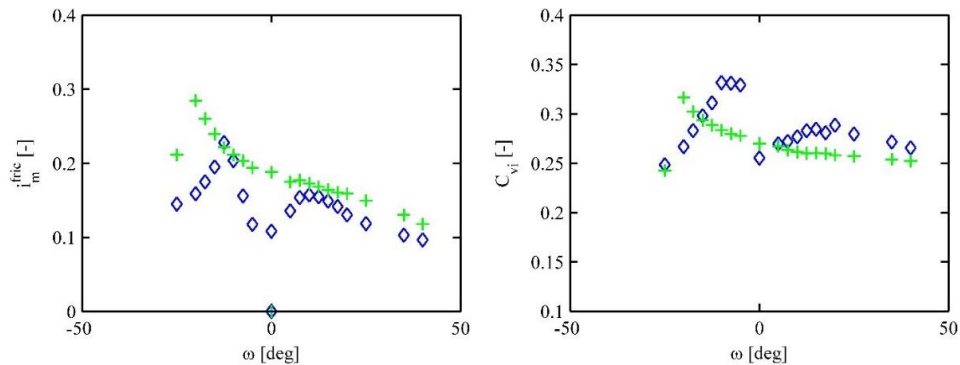


Figure 7. 5 Frictional hydraulic gradient (on the left) & Spatial volumetric concentration (on the right) in sand-water flow at $V_m \approx 2.5$ m/s and $C_{vd} \approx 0.24$ at different inclination angles, $C_{\text{mode}} = 1$.
Legend: blue diamond marker: measured friction gradient; green plus marker: IILM (two-layered model) results.

The initial tests for the friction gradient show that the model is able to capture the trend of flow behaviour while increasing or decreasing the inclination angle, however, that trend does not represent the correct values for each observation point; for all inclination angles, the model overestimates the friction gradient. The first statement remains true also for the spatial volumetric concentration, nevertheless, the C_{vi} values for each observation point are rather underestimated. This result was predictable, as the same resemblance was noticed at the experimental results of broadly-graded and narrow-graded slurry flow (for which the model works best).

I have presented in Figure 7.8. also a few examples of the modelled solids concentration profiles. Keeping the parameters constant, the two layered model is able to predict concentration profiles quite similar to real ones.

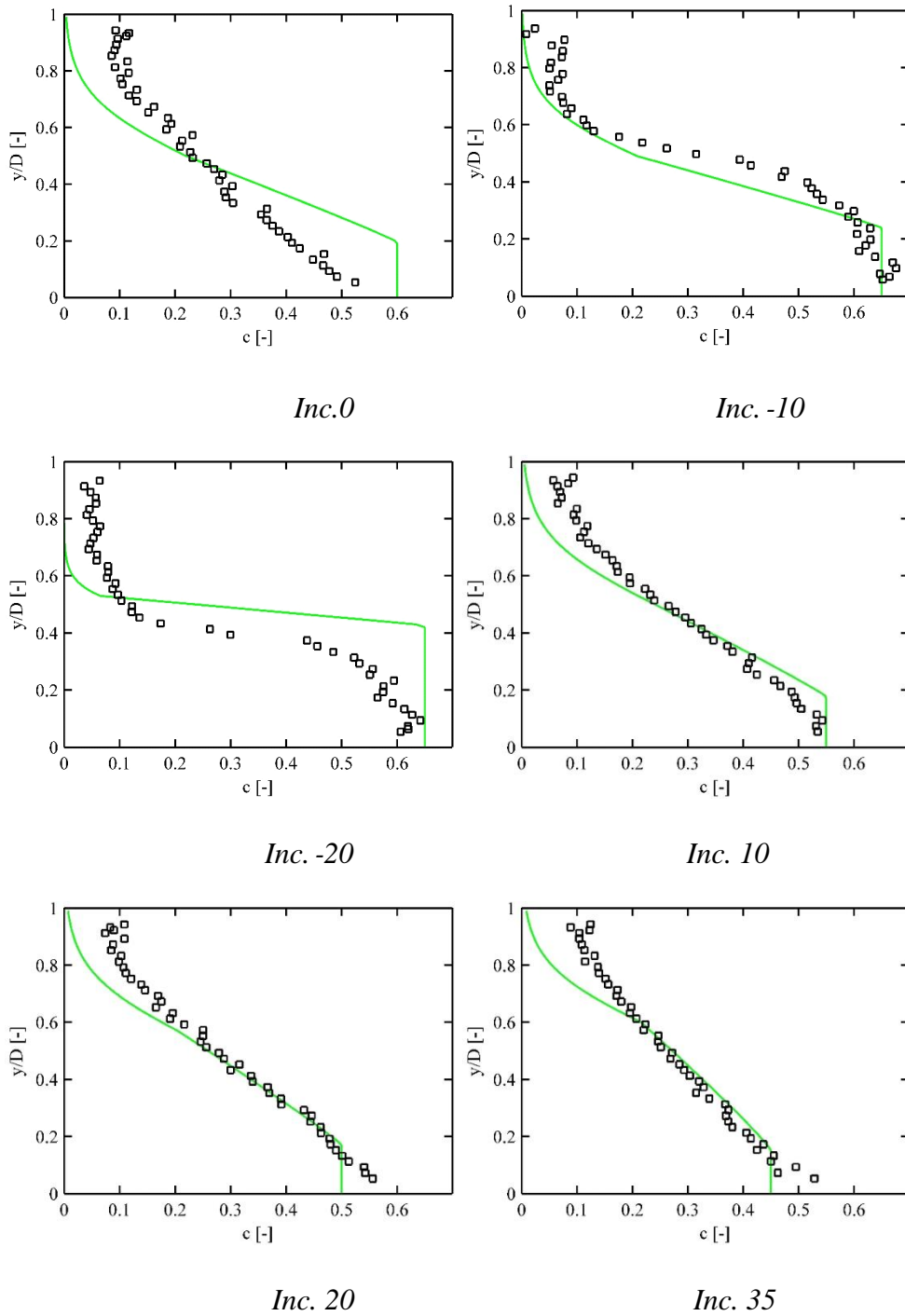


Figure 7. 6 Solids concentration profile of sand-water flow at $V_m \approx 2.5$ m/s and $C_{vd} \approx 0.24$ at different inclination angles, $C_{mode} = 1$. Legend: black square marker: measured solids concentration; green-line: modelled solids concentration.

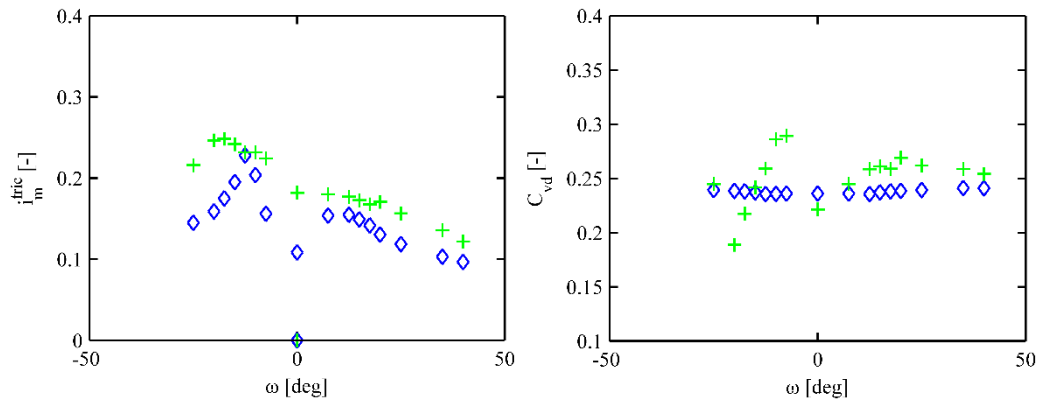


Figure 7.7 Frictional hydraulic gradient (on the left) & Spatial volumetric concentration (on the right) in sand-water flow at $V_m \approx 2.5$ m/s and $C_{vd} \approx 0.24$ at different inclination angles, $C_{\text{mode}} = 2$. Legend: blue diamond marker: measured friction gradient; green plus marker: ILM (two-layered model) results.

The other tests were run by having C_{vi} as an input to the model and C_{vd} as an output. The results are more or less similar to the previous ones, thus the change of the concentration type input is not very significant in this case.

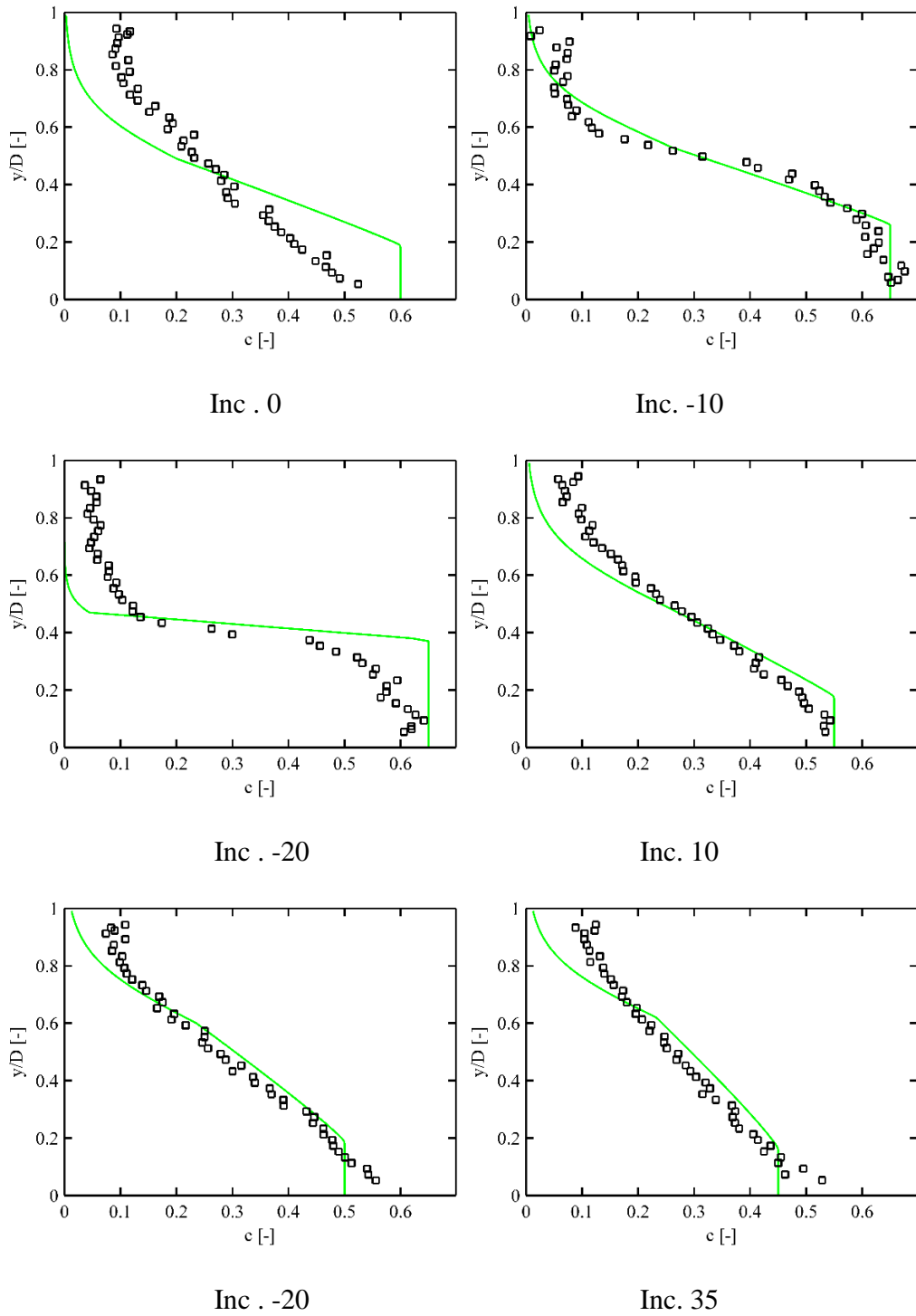


Figure 7. 8 Solids concentration profile of sand-water flow at $V_m \approx 2.5$ m/s and $C_{vd} \approx 0.24$ at different inclination angles, $C_{mode} = 2$. Legend: black square marker: measured solids concentration; green-line: modelled solids concentration.

7.2.3 Results' analysis

In the results presented below, a comparison of results for the frictional gradient and C_{vi} , predicted by various roughness' equations is performed. All the above-mentioned roughness equations were tested, and among them, only the following were fit to be used with the current data.

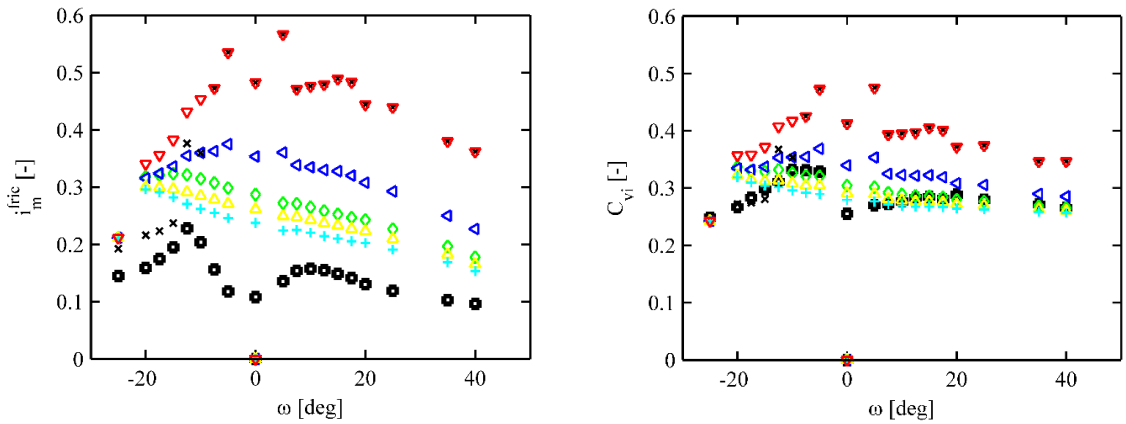


Figure 7. 9 Results for different friction gradients and spatial volumetric concentrations, of sand-water flow, at $V_m \approx 2.5$ m/s and $C_{vd} \approx 0.24$, at different inclination angles, with $transpEq = 1$; $Cmode = C_{vd}$; Legend : black-square: Measured frictional hydraulic gradient; green-diamond: fricEq= 2; blue-back-arrow: fricEq= 3; black-x: fricEq= 5; yellow-up-triangle: fricEq= 6; cyan-plus: fricEq= 9; red-down-triangle: fricEq= 10;

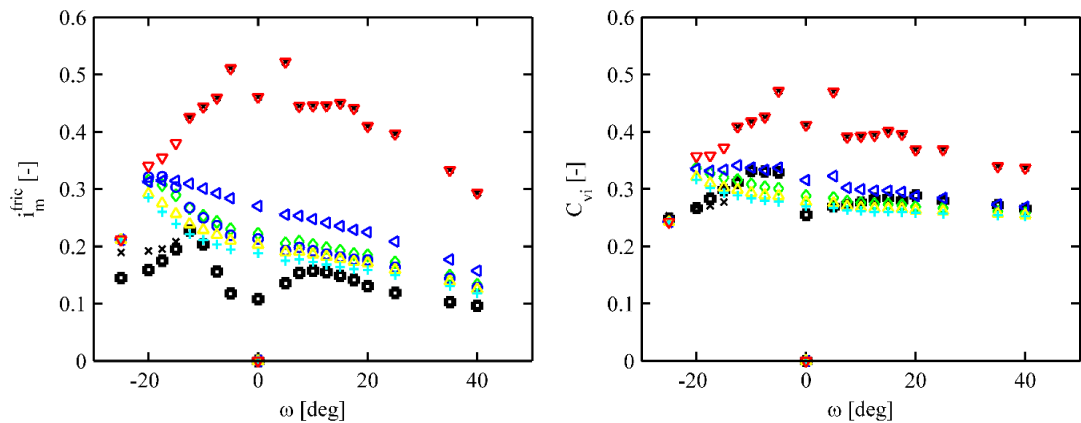


Figure 7. 10 Results for different friction gradients and spatial volumetric concentrations, of sand-water flow, at $V_m \approx 2.5$ m/s and $C_{vd} \approx 0.24$, at different inclination angles, with $transpEq = 2$; $Cmode = 1$; Legend : black-square: Measured frictional hydraulic gradient; green-diamond: fricEq= 2; blue-back-arrow: fricEq= 3; blue-circle: fricEq= 4; black-x: fricEq= 5; yellow-up-triangle: fricEq= 6; cyan-plus: fricEq= 9; red-down-triangle: fricEq= 10;

The same technique was followed to produce results of frictional gradient and the C_{vd} , while having C_{vi} as an input to the model.

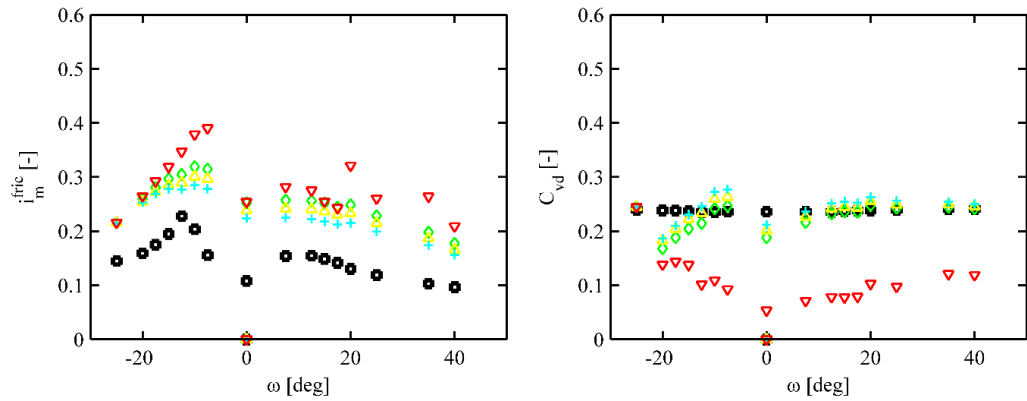


Figure 7.11 Results for different friction gradients and delivered volumetric concentrations, of sand-water flow, at $V_m \approx 2.5$ m/s and $C_{vd} \approx 0.24$, at different inclination angles, with $transpEq = 1$, $Cmode = 2$; Legend: black-square: Measured frictional hydraulic gradient; green-diamond: $fricEq = 2$; yellow-up-triangle: $fricEq = 6$; cyan-plus: $fricEq = 9$; red-down-triangle: $fricEq = 10$;

C_{vi} is an input, C_{vd} is an output. $TranspEq = 2$:

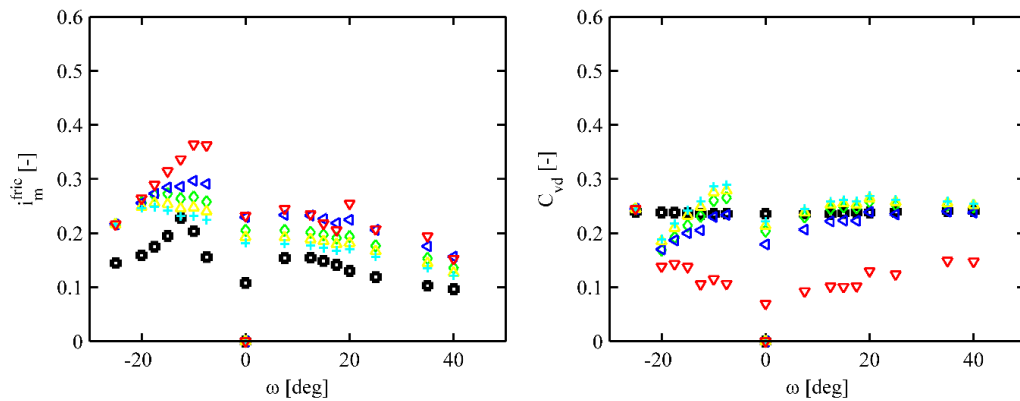


Figure 7.12 Results for different friction gradients and delivered volumetric concentrations, of sand-water flow, at $V_m \approx 2.5$ m/s and $C_{vd} \approx 0.24$, at different inclination angles, with $transpEq = 2$, $Cmode = 2$; Test with $transpEq = 2$; Legend: black-square: Measured frictional hydraulic gradient; green-diamond: $fricEq = 2$; blue-back-arrow: $fricEq = 3$; yellow-up-triangle: $fricEq = 6$; cyan-plus: $fricEq = 9$; red-down-triangle: $fricEq = 10$;

The plots presented above show the prediction results of different transport formulas, roughness coefficient formulas, as well as model sensitivity to the concentration variable. These tests were run in order to determine how to proceed, i.e. which friction equations are able to give reasonable results. Figures 7.11-7.14 show that friction equations labelled 2, 6 and 9 are best at prediction of the required variables and the model is also capable to run all data by using these equations.

7.2.4 Particle size effect to model performance

As the title of this thesis highlights, a great focus is given to the particle size diameter and how sensitive the inclined settling aqueous slurry flows are to it.

Often in slurry studies, the authors use different particle sizes in order to find which is the typical size of the tested sample and makes a better representation of it. I decided to follow this approach to understand the significance of the particle size input in the model predictions. Up to now, all the tests were made by using the mean particle size diameter (d50) to represent all the solids in the sample. Below, I will present the other predictions which show and make a comparison between model performance by using lower or higher values of solids diameter. Among a range of possible particle sizes, I chose d30 and d75 as representatives of each side of the scale. The representative values were detected through the particle size distribution curve, which is shown at the third section of this thesis:

$$d_{30} = 0.40\text{mm}$$

$$d_{50} = 0.55\text{mm}$$

$$d_{75} = 1.00\text{mm}.$$

I ran tests which cover all possible combinations of inputs of interest: concentration mode, friction roughness equation, transport equation and diameter size. Presented here are only some of the results, since it is not necessary to show all the produced plots, however, the rest are attached at the appendix section at the end of this thesis.

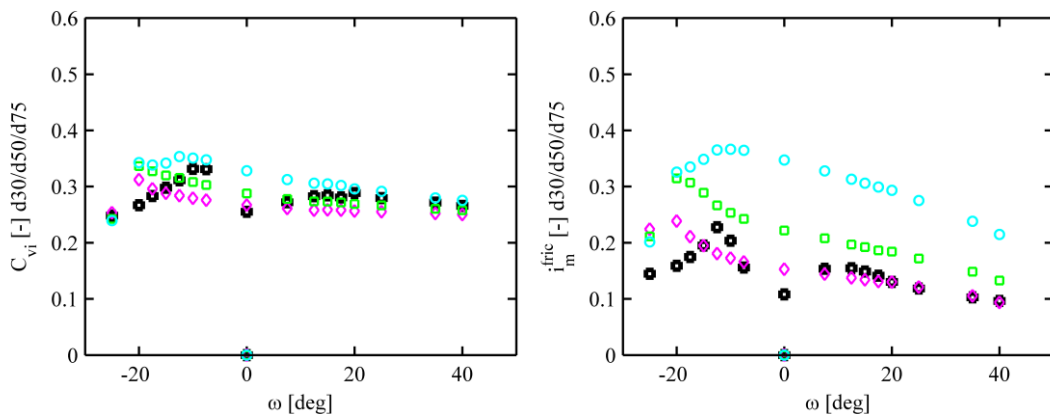


Figure 7. 13 Results for different friction gradients and delivered volumetric concentrations, of sand-water flow, at $V_m \approx 2.5$ m/s and $C_{vd} \approx 0.24$, at different inclination angles, with $transpEq = 2$, $Cmode = 1$, $fricEq 2$; Legend: black-square Measured frictional hydraulic gradient/ C_{vi} ; green-square: d50; magenta-diamond: d30; cyan-circle: d75.

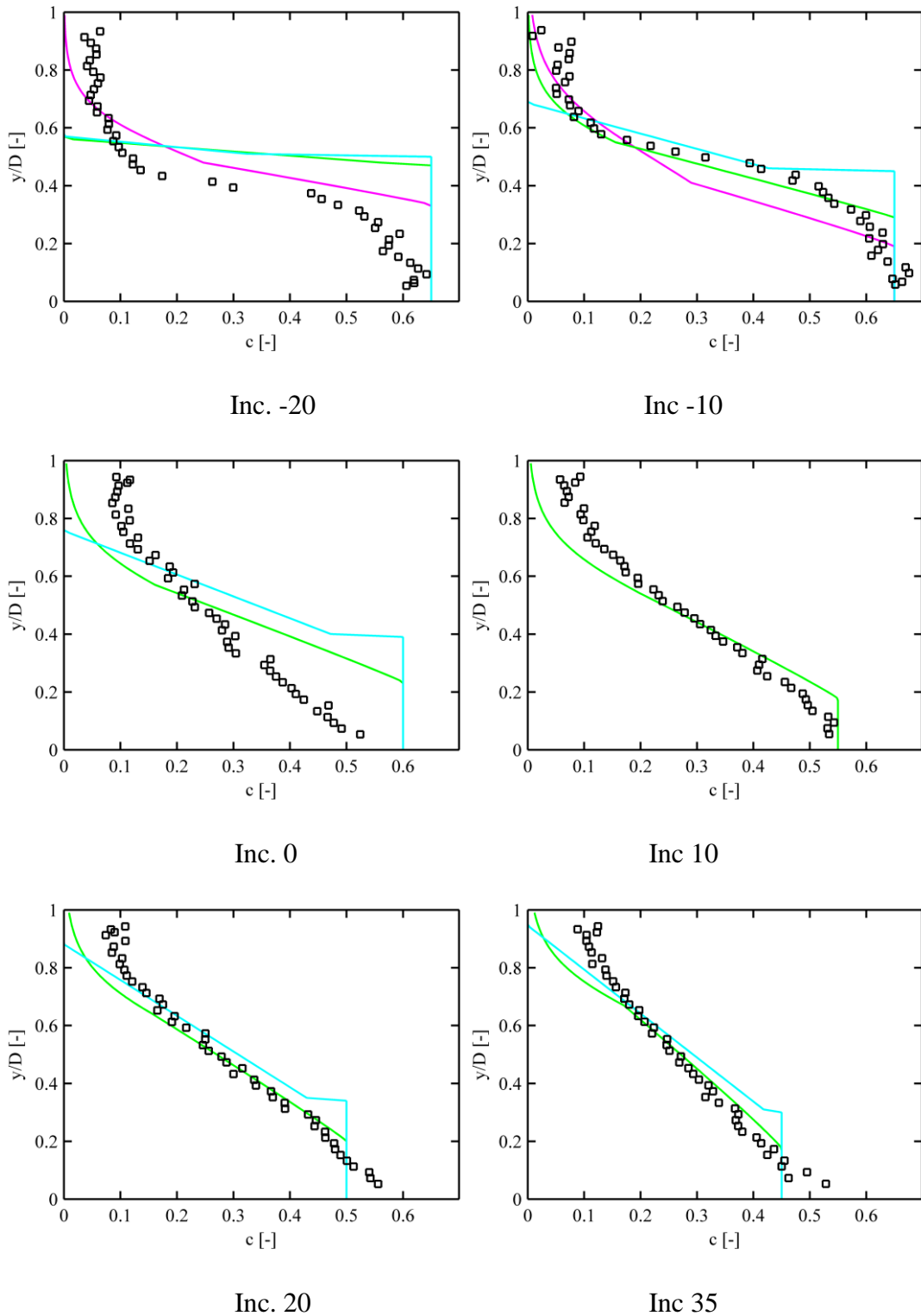


Figure 7. 14 Solids concentration profile of sand-water flow at $V_m \approx 2.5$ m/s and $C_{vd} \approx 0.24$ at different inclination angles, with $transpEq = 2$, $Cmode = 1$, $fricEq 2$; Legend: black-square: measured concentration profile; green-square: d_{50} ; magenta-diamond: d_{30} ; cyan-circle: d_{75} .

The Matoušek model with the delivered concentration as an input and the spatial concentration as an output was used to get the results presented in the Figure 7.15 and Figure 7.16. The proposed correlations of the transport equation from Matoušek and

Krupička (2014) and the roughness equation from Matoušek (2003) were utilized and the results are considered satisfying. The application of different characteristic grain size shows different results, therefore, confirming that the particle size is a very important variable for the model. The model is able to capture the trend of the friction gradient curve and the concentration curve for all particle diameters used as the characteristic grain size of the sample. The model considers the diameter input as the mean value of a sample and is not able to recognize how widespread the PSDC is. Considering the d30 as the characteristic grain size, the model recognizes a sample of very fine sand; while it is not capable to calculate many concentration profiles, the ones that are produced show a very realistic picture of the concentration. The concentration profile estimated by using this diameter size shows a smoother curve of solids distribution in the pipe cross-section, which is exactly what happens in the broadly graded slurries. On the other hand, usage of a much higher diameter size, such as d75, produces unrealistic concentration profiles, since the model considers the sample as coarse sand. The prediction of friction gradient and the spatial concentration are satisfactory; however, the usage of this characteristic particle size produces the worst results in my tests. Considering d50 as the characteristic diameter of the sample, as it is conventionally used, the model is able to predict quite accurate friction gradient and spatial concentrations for different inclination angles. The solids distribution predicted by the model while using the d50 is not as good as d30, but the model is able to produce these profiles for all the required inclination angles.

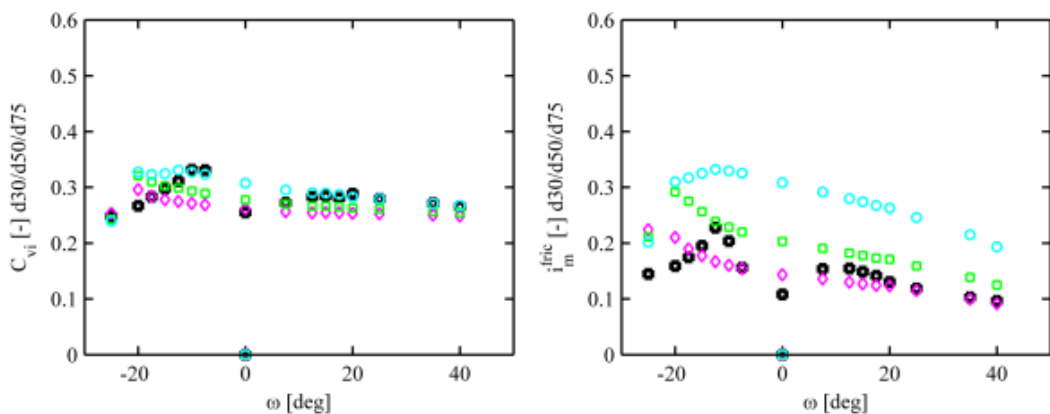


Figure 7. 15 Results for different friction gradients and delivered volumetric concentrations, of sand-water flow, at $V_m \approx 2.5$ m/s and $C_{vd} \approx 0.24$, at different inclination angles, with $transpEq = 2$, $Cmode = 1$, $fricEq = 6$; Legend: black-square Measured frictional hydraulic gradient/ C_{vi} ; green-square: d50; magenta-diamond: d30; cyan-circle: d75

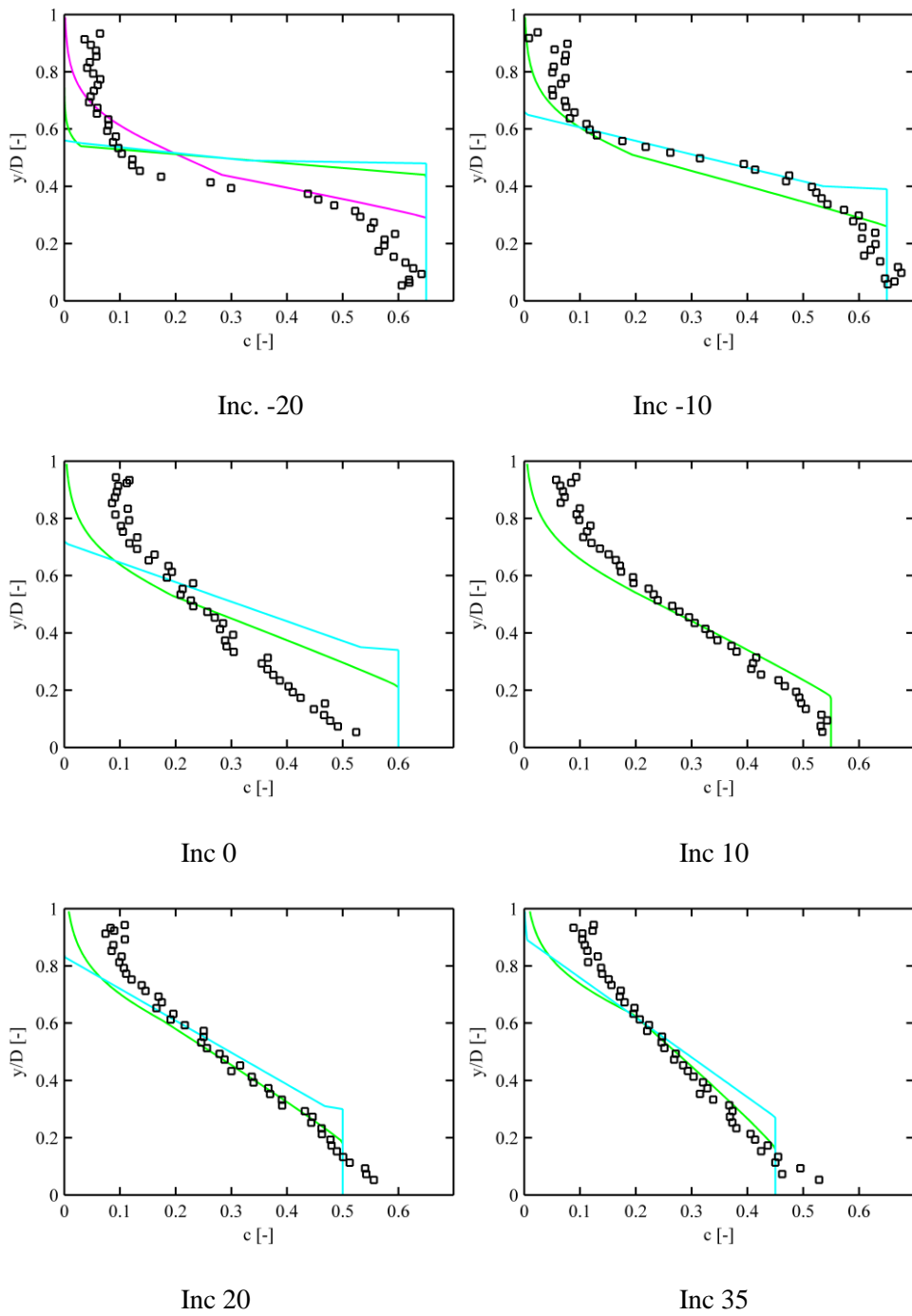


Figure 7. 16 Solids concentration profile of sand-water flow at $V_m \approx 2.5$ m/s and $C_{vd} \approx 0.24$ at different inclination angles, with $transpEq = 2$, $Cmode = 1$, $fricEq = 6$; Legend: black-square: measured concentration profile; green-square: d50; magenta-diamond: d30; cyan-circle: d75.

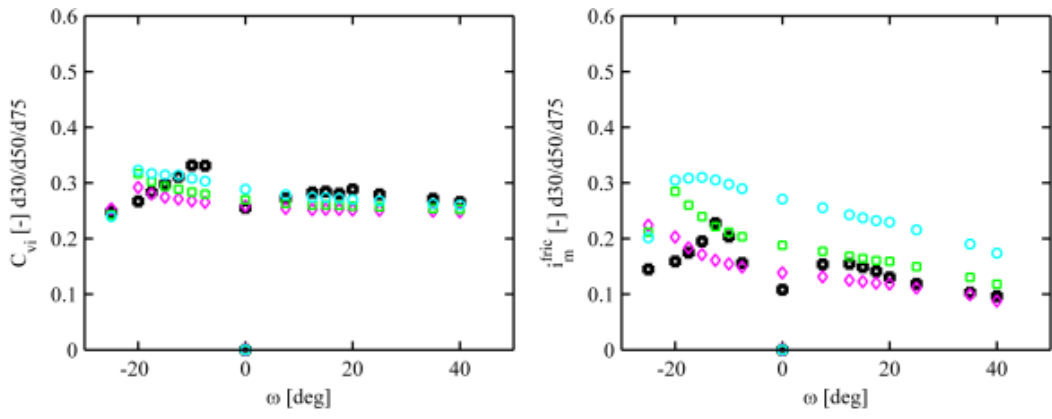


Figure 7. 17 Results for different friction gradients and delivered volumetric concentrations, of sand-water flow, at $V_m \approx 2.5$ m/s and $C_{vd} \approx 0.24$, at different inclination angles, with $transpEq = 2$, $C_{mode} = 1$, $fricEq = 9$; Legend: black-square Measured frictional hydraulic gradient/ C_{vi} ; green-square: d50; magenta-diamond: d30; cyan-circle: d75.

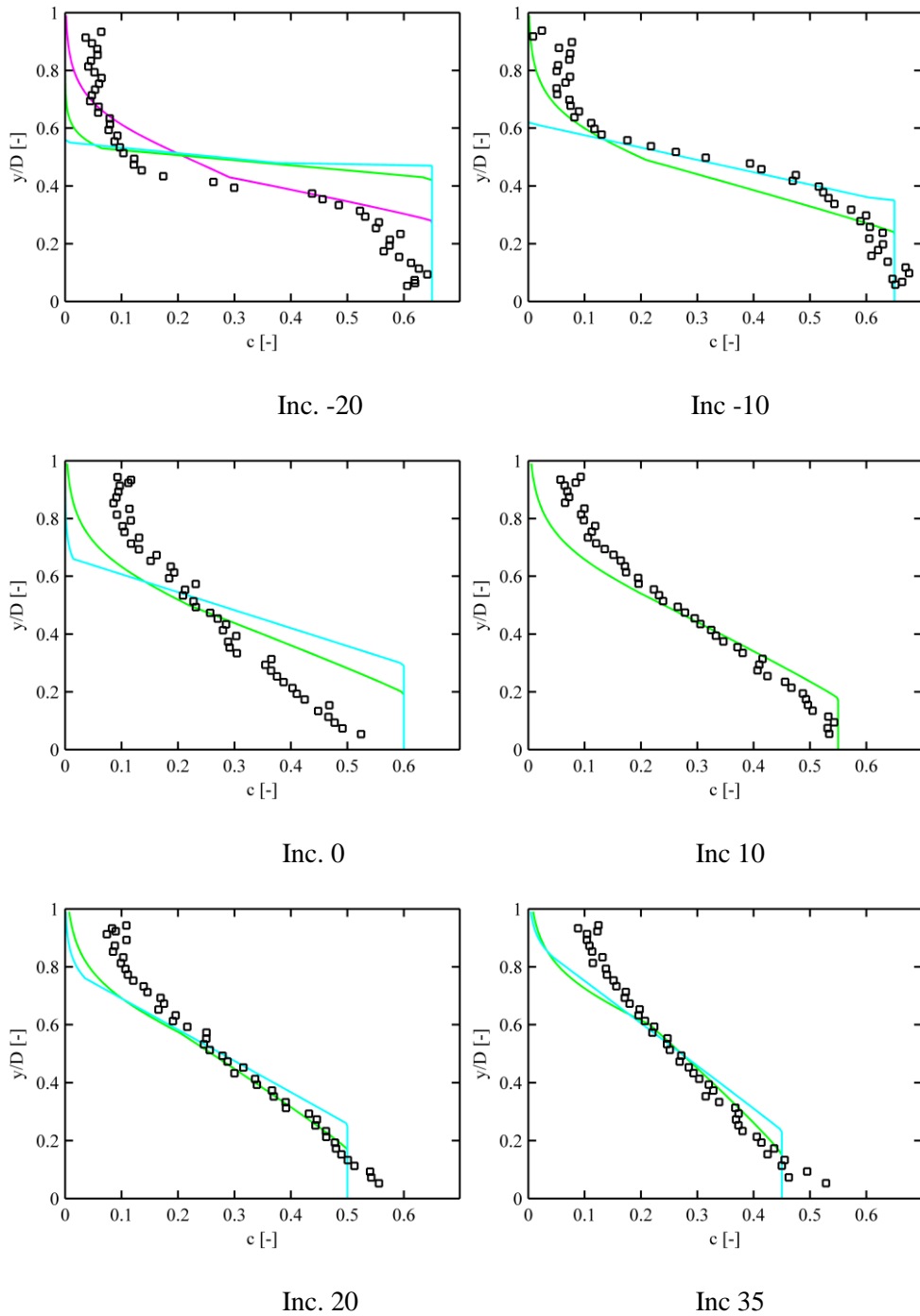


Figure 7. 18 Solids concentration profile of sand-water flow at $V_m \approx 2.5$ m/s and $C_{vd} \approx 0.24$ at different inclination angles, with $transpEq = 2$, $Cmode = 1$, $fricEq 9$; Legend: black-square: measured concentration profile; green-square: d_{50} ; magenta-diamond: d_{30} ; cyan-circle: d_{75} .

Even though the performance of the model in each case is clear from the plots, I have evaluated the ME (mean error) for each observation point and put the final results in the table below. I selected a simple form of error evaluation because it is relevant in this case. Also, I found it more interesting to neglect any absolute value or square value calculation of the errors, because the final sign matters, especially when evaluating the

pressure gradient: if the average error has a positive sign, it shows that the model is underestimating the pressure gradient, on the other hand if the average error has a negative sign, it shows that the model is overestimating the pressure gradient in the pipe. In the process of designing a pipeline, it is always important to choose the safer version, which in this case would be an overestimation of pressure losses.

$$ME = \frac{1}{n} \left(\sum_{i=1}^n x_{meas} - x_{mod} \right) \quad (24)$$

Test :	Cmode 1					
i_fric	TranspEq 1			TranspEq2		
ME	d30	d50	d75	d30	d50	d75
fricEq 2	-0.0671	-0.1162	-0.1784	-0.0075	-0.0695	-0.1567
fricEq 6	-0.0517	-0.0959	-0.1507	0.0027	-0.0517	-0.1291
fricEq 9	-0.0426	-0.0787	-0.1223	0.0073	-0.0395	-0.1031

Test :	Cmode 2					
i_fric	TranspEq 1			TranspEq2		
ME	d30	d50	d75	d30	d50	d75
fricEq 2	-0.0652	-0.1055	-0.1507	-0.0114	-0.0652	-0.1330
fricEq 6	-0.0545	-0.0930	-0.1364	-0.0024	-0.0531	-0.1181
fricEq 9	-0.0470	-0.0804	-0.1185	0.0017	-0.0431	-0.1011

Table 7. 1 Frictional hydraulic gradient mean error (measured vs. modelled) for 10 mm pipe test of sand-water flow at $V_m \approx 2.5$ m/s and $C_{vd} \approx 0.24$.

Test :	Cmode 1					
Cv_i/d	TranspEq 1			TranspEq2		
ME	d30	d50	d75	d30	d50	d75
fricEq 2	0.0007	-0.0130	-0.0331	0.0154	-0.0026	-0.0288
fricEq 6	0.0086	-0.0022	-0.0175	0.0212	0.0069	-0.0136
fricEq 9	0.0129	0.0058	-0.0040	0.0236	0.0130	-0.0010

Test :	Cmode 2					
Cv_i/d	TranspEq 1			TranspEq2		
ME	d30	d50	d75	d30	d50	d75
fricEq 2	-0.0008	0.0133	0.0351	-0.0154	0.0026	0.0302
fricEq 6	-0.0089	0.0022	0.0181	-0.0215	-0.0071	0.0140
fricEq 9	-0.0132	-0.0060	0.0040	-0.0240	-0.0134	0.0010

Table 7. 2 Distributed/Spatial volumetric concentration mean error (measured vs. modelled) for 10 mm pipe test of sand-water flow at $V_m \approx 2.5$ m/s and $C_{vd} \approx 0.24$.

7.2.5 Findings

- In general, the usage of d30 in the calculations, produces less errors in the frictional gradient prediction.
- Usage of d30 also gives a better performance of the model to predict the concentration profiles, but since the sand particles are considered so small, in many inclination angles, the model is unable to produce one.
- Using d75 produces the least realistic profile concentrations of solids in the pipe.
- These statements are also supported by the detection of smaller errors of concentration calculations when using d30 or d50.
- This suggests that d50 is the best-inclusive diameter to be used.
- Transport equation nr.2 (Krupička, 2014) gives a better prediction of the frictional gradient, while Transport equation nr.1 (Matoušek, 2009) gives a better prediction of the solids' concentration.
- Cmode 1 and Cmode 2 are quite similar, however, the metrics show a better performance of the model by using Cmode1.
- By using friction equation nr. 9, the model performs better as for the frictional gradient.
- The friction equation nr. 6 is better at estimating the concentration of solids.

8 Conclusions and Recommendations

Overall, the scope of this research was to determine the effect of particle size distribution in the pressure drop for inclined slurry flow. Experimental study shows that the solids' grading affects the slurry flow behaviour in all inclinations. The comparison between broadly and narrow graded slurry reveals that despite having the same mean particle size, the broadly graded slurry exhibits less friction and therefore both frictional and manometric pressure losses are less than in the narrow-graded one. Similar to the narrow-graded slurry flow, an anomalous pressure drop is identified in the mild negative slopes, however, less evident in the broadly graded slurry.

The Worster-Denny formula for estimating the frictional gradient is almost incapable of predicting accurate results in the inclined pipe flows. The Worster-Denny formula underestimates the frictional component of the pressure gradient especially in mild inclination angles. Various modifications made to the original formula show that the friction gradient is highly dependent on the spatial volumetric concentration, therefore it is recommended to include this parameter in the formula.

The two-layered model is able to predict the trend of frictional gradient in a range of different inclination angles. However, the tests conducted in this timeframe with a set of roughness coefficient formulas show that all of them need further modifications to produce more precise results. In general, the best friction equation suggested for use is friction equation nr. 9, which has been constantly calibrated on data from IH Prague. Transport equations 1 and 2 give similar results, however the second shows a slightly better performance. The two-layered model performance is improved when using the delivered spatial concentration C_{vd} as an input.

Particle size distribution curve is an important tool for describing the solids of a given sample. Although the mean particle size, d_{50} , can be generally considered the best option, for broadly graded slurry flow, the concentration profiles produced by using a smaller diameter size are closer to reality. Unfortunately, the model cannot produce complete results for the concentration profiles, when using a smaller diameter, such as d_{30} , and this remains to be analysed and studied in the future. Using d_{30} to calculate friction pressure losses gives worse results than using d_{50} . On the other hand, using a higher diameter size, such as d_{75} , produces unrealistic concentration profiles, and it tends to overestimate the friction gradient and the volumetric concentrations. The

model, in its current state, reaches its peak performance by using d_{50} in the calculations.

As this thesis is a continuation of relentless work of researchers all over the globe, but especially from the research team of Institute of Hydrodynamics in Prague, I will divide what I see as necessary steps further in two directions.

Throughout the years, the research team at IH Prague has managed to carry out a number of experiments regarding different slurry flows and has developed a two layered model which predicts the slurry behaviour in different inclinations. All models always have place for improvements in order to be more efficient and widely applicable. I tested the existing model utile for slurry flows of broadly graded sand, and the results are satisfying. Currently, the model is not able to predict pressure losses or solids' distribution profiles in inclinations steeper than -25 degrees, because the concept of force balance changes at those higher inclination angles. The bed at the bottom of the pipe slides really fast, and its velocity exceeds the mean velocity in the pipe. In this situation, it is necessary to make force balance analysis and add another condition to the model for that particular range of inclination angles (ideally, the model has to understand automatically when to switch the condition).

Going back to the global perspective, I want to mention a problem which I encountered during the experiments but was not mentioned because it is not within the scope of this thesis. Despite the tests at mean velocity 2.5 m/s, I ran tests at higher and lower mean velocities, which brought attention to the phenomenon of turbulence. When the mean velocity in the flow reaches lower values (in these particular tests, below say 1.7 m/s), the flow becomes unstable and turbulence develops. This becomes significantly important since the industry pipelines usually run at the lowest-possible/critical velocities in order to be energy efficient and to save the composition of their carrying mixture. Initiation of turbulence in pipelines carrying solids in large proportions could disturb the flow and clog the pipe. Comparing to previous research, a higher occurrence of turbulence is observed in experiments with narrow-graded materials; therefore, it can be stated that broadly graded slurries are much safer to be transported.

9 References

- Albar, A. (2000). Effect of various terminal velocity equations on the result of friction loss calculation. *Terra et Aqua*, pp.13-21.
- Camenen, B., Bayram, A., & Larson, M. (2006). Equivalent roughness height for plane bed under steady flow. *Journal of Hydraulic Engineering*, 132(11), pp. 1146-1158.
- Craig, R. F. (2004). *Craig's soil mechanics seventh edition*. London: Spon Press.
- Durand, R., & Condolios, E. (1952). Experimental study of the hydraulic transport of coal and solid material in pipes. In *Proc. Colloq. on the Hydraulic Transport of Coal, Natl. Coal Board, UK*, pp. 39-55.
- Garcia, M. H. (2008). Sediment Transport and Morpho Dynamics. In *Sedimentation engineering: Processes, measurements, modeling, and practice* pp. 21-163. AsceLibrary.
- Gillies, R. G., & Shook, C. A. (1991). Deposition velocity correlation for water slurries. *The Canadian Journal of Chemical Engineering*, 69(5), pp. 1225-1227.
- Jovanović, M., & Matoušek, V. (2019). The effect of longitudinal slope on solids transport and friction in particle-laden flow above stationary deposit in pipe. In: *Proc. 19th Int. Conference on Transport & Sedimentation of Solid Particles, 27-79 September, Cape Town*, pp. 137-144. Wrocław University of Environmental and Life Sciences.
- Krupička, J. (2014) *Mathematical and Physical Modelling of Pipe Flow of Settling Slurries*. [Doctoral dissertation]. Czech Technical University in Prague, Czech Republic.
- Lahiri, S. K., & Ghanta, K. C. (2009). Computational fluid dynamics simulation of solid-liquid slurry flow. *Hydrocarbon Processing*, 88(4), pp. 99-104.
- Matoušek, V. (1997) *Flow mechanism of sand-water mixtures*. [Doctoral dissertation]. Delft University of Technology, The Netherlands.

- Matoušek, V. (2003). Effect of solids distribution near a pipe wall on flow friction in a slurry pipeline. In *Proc. The 4th Int. Conf. for Conveying and Handling of Particulate Solids, Budapest*, pp. 13.19-13.24.
- Matoušek, V. (2009). Predictive model for frictional pressure drop in settling-slurry pipe with stationary deposit. *Powder Technology*, 192(3), pp. 367-374.
- Matoušek, V. (2019). Settling Slurries Advanced Topics. *42nd Annual Slurry Course* [Conference Presentation]. GIW Industries.
- Matoušek, V. & Krupička, J. (2008). On hydraulic roughness of top of stationary bed in pressurized pipes. In *Proc. 14th Int. Conference on Transport & Sedimentation of Solid Particles, St. Petersburg*, pp. 213-221.
- Matoušek, V., & Krupička, J. (2010). Modeling of settling-slurry flow around deposition-limit velocity. In *Proc. Hydrotransport*. pp.143-154.
- Matoušek, V., & Krupička, J. (2014). Interfacial friction and transport in stratified flows. In *Proceedings of the Institution of Civil Engineers-Maritime Engineering*. Thomas Telford Ltd. pp. 125-134.
- Matousek, V., & Zrostlik, S. (2019). Testing of criterion for local turbulent support of grains in sheet flow layer. *EGU General Assembly Conference Abstracts*, Vol. 21, pp.1.
- Matoušek, V., Konfršt, J., Krupička, J., & Vlasák, P. (2019). Anomalous pressure drop in settling slurry flow through pipe of mild negative slope. In *Proc. 19th Int. Conference on Sedimentation and Transportation of Solid Particles, Cape Town, RSA*. pp. 161-168. Wrocław University of Environmental and Life Sciences.
- Matoušek, V., Krupička, J., & Kesely, M. (2018). A layered model for inclined pipe flow of settling slurry. *Powder Technology*, 333, pp. 317-326.
- Miedema, S., & Ramsdell, RC. (Ed.) (2016). *Slurry Transport: Fundamentals, a historical overview and the Delft Head Loss & Limit Deposit Velocity Framework*. (1st ed.) Delft, The Netherlands: SA Miedema / Delft. University of Technology.

- Miedema, S.A. (2019). *DHLLDV Framework, Inclined Pipes*. [Conference Presentation]. The Delft Head Loss & Limit Deposit Velocity Framework.
- Newitt, D.M., Richardson, J.F., Abbott, M., & Turtle, R.B. (1955). Hydraulic Conveying of Solids in Horizontal Pipes. *Transactions of the Institution of Chemical Engineers*, 33, pp. 93-113.
- Polanský, J. (2014). *Experimental investigation of slurry flow*. [Doctoral Thesis], University of Leeds. CZ.1.07/2.3.00/20.0139.
- Rayner, R. (1995). *Pump users handbook*. Elsevier.
- Shook, C.A., Gillies, R.G., & Sanders, R.S. (2002). *Pipeline Hydrotransport: With Applications in the Oil Sand Industry*. SRC Pipe Flow Technology Center.
- Sumer, B. M., Kozakiewicz, A., Fredsøe, J., & Deigaard, R. (1996). Velocity and concentration profiles in sheet-flow layer of movable bed. *Journal of Hydraulic Engineering*, 122(10), pp. 549-558.
- US Soil Conservation Service. (1983). National Engineering Handbook: Sedimentation. In *U.S. Department of Agriculture, Soil Conservation Service*.
- Visintainer, R. J., Furlan, J. M., McCall, G., Sellgren, A., & Matoušek, V. (2017). Comprehensive loop testing of a broadly graded (4-component) slurry. In *20th International Conference on Hydrotransport, Melbourne, Australia, 3-5 May 2017*. pp. 307-323. BHR Group Limited.
- Wilson, K. C., & Pugh, F. J. (1988). Dispersive-force modelling of turbulent suspension in heterogeneous slurry flow. *The Canadian Journal of Chemical Engineering*, 66(5), pp. 721-727.
- Wilson, K. C., Addie, G. R., Sellgren, A., & Clift, R. (2006). *Slurry transport using centrifugal pumps*. Springer Science & Business Media.
- Worster, R. C., & Denny, D. F. (1955). Hydraulic transport of solid material in pipes. *Proceedings of the Institution of Mechanical Engineers*, 169(1), pp. 563-586.
- Yalin, M. S. (2015). *River mechanics*. Elsevier.